Title: Hypertriglyceridemia as a Key Contributor to Abdominal Aortic Aneurysm Development and Rupture: Insights from Genetic and Experimental Models

Author: Yaozhong Liu[1], Huilun Wang[1,2], Minzhi Yu[3], Lei Cai[4], Ying Zhao[1], Yalun Cheng[1], Yongjie Deng[1], Yang Zhao[1], Haocheng Lu[5], Xiaokang Wu[1], Guizhen Zhao[1,6], Chao Xue[1,7], Hongyu Liu[1], Ida Surakka[1], Anna Schwendeman[3], Hong S. Lu[4], Alan Daugherty[4], Lin Chang[1], Jifeng Zhang[1], Ryan E. Temel[4,*], Y. Eugene Chen[1,8,*], Yanhong Guo[1,*]

[1]Department of Internal Medicine, Frankel Cardiovascular Center, University of Michigan Medical Center, Ann Arbor, Michigan, USA.

[2]Department of Molecular Physiology and Biological Physics, University of Virginia School of Medicine, Charlottesville, Virginia, USA.

[3]Department of Pharmacology, University of Michigan, Ann Arbor, Michigan, USA.

[4]Saha Cardiovascular Research Center and Department of Physiology, College of Medicine, University of Kentucky, Lexington, Kentucky 40536.

[5]Department of Pharmacology, Southern University of Science and Technology, Guangdong, China.

[6]College of Pharmacy Health, University of Houston, Houston, Texas, USA.

[7]Department of Internal Medicine, Rochester General Hospital, Rochester, New York, USA.

[8]Center for Advanced Models for Translational Sciences and Therapeutics, University of Michigan Medical Center, Ann Arbor, Michigan, USA.

Total word count: 11587

*** To whom correspondence should be addressed:**

Yanhong Guo, M.D., Ph.D., Department of Internal Medicine, University of Michigan Medical Center, Ann Arbor, MI 48109, Phone: 734-764-1405, Email: yanhongg@umich.edu

Or

Y. Eugene Chen, M.D., Ph.D., Department of Internal Medicine, University of Michigan Medical Center, Ann Arbor, MI 48109, USA. Phone: 734-936-9548, Email: echenum@umich.edu

Or

Ryan E. Temel, Ph.D., Saha Cardiovascular Research Center and Department of Physiology, College of Medicine, University of Kentucky, Lexington, KY 40536, USA. Phone: 859-218-1706, Email: ryan.temel@uky.edu

Abstract:

Abdominal aortic aneurysm (AAA) is a life-threatening vascular disease without effective medications. This study integrated genetic, proteomic, and metabolomic data to identify causation between increased triglyceride (TG)-rich lipoproteins and AAA risk. Three hypertriglyceridemia mouse models were employed to test the hypothesis that increased plasma TG concentrations accelerate AAA development and rupture. In the angiotensin II-infusion AAA model, most *Lpl*-deficient mice with severely high plasma TG concentrations died of aortic rupture. Consistently, *Apoa5*-deficient mice with moderately increased TG concentrations had accelerated AAA development, while human *APOC3* transgenic mice with dramatically increased TG concentrations exhibited aortic dissection and rupture. Increased TG concentrations and palmitate inhibited lysyl oxidase maturation. Locally overexpressing lysyl oxidase eliminated the impact of high TG on AAA formation in human *APOC3* transgenic mice. Administration of antisense oligonucleotide targeting *Angptl3* profoundly inhibited AAA progression in human *APOC3* transgenic mice and *Apoe*-deficient mice. These results indicate that hypertriglyceridemia is a key contributor to AAA pathogenesis, highlighting the importance of triglyceride-rich lipoprotein management in treating AAA.

Clinical Perspective

What Is New?

- This study integrates genetic, proteomic, and metabolomic data to identify causation between increased triglyceride (TG)-rich lipoproteins and AAA risk.
- TG concentrations influence AAA formation and severity in a dose-dependent manner, potentially by inhibiting lysyl oxidase maturation and extracellular matrix assembly.
- Administration of antisense oligonucleotide targeting *Angptl3* profoundly inhibites AAA progression in human *APOC3* transgenic mice and *Apoe*-deficient mice by lowering TG concentrations.

What Are the Clinical Implications?

- These findings underscore triglyceride-rich lipoprotein management as a promising therapeutic strategy for AAA treatment.
- Antisense oligonucleotide therapy targeting liver ANGPTL3 holds potential as a therapeutic approach to reduce AAA risk.

Introduction

Abdominal aortic aneurysm (AAA) is a progressive vascular disease characterized by the localized enlargement of the abdominal aorta. The prevalence of AAA is estimated to be as high as 8% in men and 2% in women over 65 years of age.[1] Most AAAs are asymptomatic, but the mortality rate is up to 80% if rupture occurs.[2] As maximum aortic diameter is the most established predictor of aneurysm rupture, current guidelines recommend considering surgical repair for asymptomatic AAA patients when maximal aortic diameter is ≥ 50 mm in women and ≥ 55 mm in men. Open surgical or percutaneous endovascular aneurysm repair is still the only therapeutic option.[3] Patients with AAA smaller than these thresholds are typically monitored through imaging surveillance. AAA-relevant risk factors, including smoking, male sex, aging, hypertension, and hyperlipidemia, are associated with enhanced aneurysm formation and growth. Currently, medications to reduce AAA risk factors, such as angiotensin II (AngII) receptor antagonists, beta-adrenoceptor blockers, statins, and anticoagulants, have not been proven effective in halting the growth of an aneurysm or preventing the rupture of asymptomatic AAA based on the findings from randomized controlled trials.[4, 5]

Our recent comprehensive genome-wide association studies (GWAS) meta-analysis, which included approximately 40,000 individuals with AAAs and over 1 million individuals without AAAs, has demonstrated that one-third of the lead variants at the 121 genome-wide significant AAA risk loci are associated with major-lipid fractions, such as total cholesterol (TC), triglycerides (TG), low-density lipoprotein cholesterol (LDL-C), or high-density lipoprotein cholesterol (HDL-C).[6] Other genetic association studies have identified that a 1-standard deviation increase in TG concentrations is associated with a 69% higher risk of AAA.[7, 8] Population-based studies have reported that individuals with increased serum very low-density lipoprotein-cholesterol (VLDL-C) and TG concentrations are more likely to develop larger AAA sizes and have a higher risk of rupture.[9, 10] These epidemiologic and genetic findings suggest that increased TG-rich lipoproteins (TRL) may accelerate AAA development and rupture, and modulating TG concentrations or metabolites may become new therapeutic strategies for AAA.

TG, also known as triacylglycerols (TAG), are composed of glycerol and fatty acids and are the most abundant lipids in the body. Chylomicrons transport dietary triglycerides from the small intestines, and VLDLs transport endogenously synthesized triglycerides from the liver to peripheral tissues, such as the heart, skeletal muscle, and adipose tissues. Triglyceride metabolism is a complex process involving the breakdown and utilization of this lipid. Several proteins and enzymes play critical roles in regulating triglyceride metabolism.[11] Among these, lipoprotein lipase (LPL), ApoC-III

(apolipoprotein C-III, APOC3), ApoC-II, ApoA-V (apolipoprotein A5, APOA5), and angiopoietin-like proteins (ANGPTL3, ANGPTL4, and ANGPTL8) are key players. LPL is a critical enzyme that facilitates the hydrolysis of triglycerides carried by chylomicrons and VLDL into free fatty acids (FFA) and glycerol, allowing them to be utilized by various cells for energy or storage. Our previous study found that an intronic LPL variant, associated with increased LPL expression, was strongly related to reduced plasma TG concentrations and AAA risk.[6] APOA5 is almost exclusively expressed in the liver and secreted in conjunction with VLDL particles. ApoC-III is a constituent of chylomicrons and VLDL particles and inhibits LPL activity, while ApoA-V and ApoC-II enhance LPL activity and promote the clearance of TG-rich lipoproteins. ANGPTL3 and ANGPTL8 are secreted proteins and inhibitors of LPL-mediated plasma TG clearance. In numerous studies involving humans and animals, loss-of-function of APOC2 or APOA5 is associated with increased plasma concentrations of TG and chylomicronemia.[12, 13] Among the putatively causal circulating proteins associated with AAA, we identified that higher APOA5 expression is significantly associated with decreased AAA risk.[6] Currently, gene silencing of APOC3 or ANGPTL3 significantly reduced TG and TC concentrations, making this method an effective strategy for lowering plasma lipids and preventing cardiovascular diseases.[14-17] In the present study, we demonstrated that increased TG-rich lipoproteins accelerate AAA formation and rupture, and we provide evidence that effective management of plasma TG concentrations can alleviate AAA progression.

Methods

The data, analytic methods, and codes will be made available to other researchers for reproducing from the corresponding author upon reasonable request. A detailed description of the methods is available in the Supplemental Materials. All genetic data used in this study were obtained from publicly available consortiums. The RNAseq original data generated during this study will be deposited in a publicly accessible database upon publication of the manuscript. All animal procedures followed the protocols approved by the Institutional Animal Care & Use Committee (IACUC) at the University of Michigan and University of Kentucky.

Statistic analysis

Analyses of RNA sequencing and genetic data were performed using R language (v4.3.0). Statistical analyses of other data were conducted using GraphPad Prism 10. Most of the data are presented as mean ± standard error of the mean (SEM). The distribution of data was assessed using the Kolmogorov-Smirnov test (for $n > 4$) or the Shapiro-Wilk test (for $n \leqslant 4$). For normally distributed data, Student's t-tests were used

158 to compare two groups, one-way analysis of variance (ANOVA) was used to compare
159 multiple groups, and the Sidak method was applied for multiple comparison correction.
160 For non-normally distributed data, Mann-Whitney U tests were used to compare two
161 groups, Kruskal-Wallis tests were employed to compare multiple groups, and the Dunn
162 method was used for multiple comparisons correction. A *P*-value less than 0.05 was
163 considered statistically significant.

164 **Results**

165 **Genetic, proteomic, and metabolic studies underscore high triglyceride-rich**
166 **lipoproteins as a causal risk factor for AAA.**
167 Genetic variants that modulate the expression of genes encoding the candidate proteins
168 or the abundances of metabolites represent valuable tools for guiding therapeutic
169 strategies. Recent studies have identified cis-acting protein quantitative trait loci (cis-
170 pQTL) that can be used as instrumental variables (IVs) for inferring causality.[18, 19]
171 Combining cis-pQTL and GWAS findings, we performed Mendelian randomization (MR)
172 analyses to assess the causal effects of circulating proteins on AAA risk and identified
173 that 41 out of 2,698 circulating proteins were significantly associated with AAA after
174 adjusting for multiple tests (Fig 1, full MR results in Supplementary Table 1). Among
175 them, genetically determined circulating APOC3 (OR=1.84, 95% CI [1.66-2.04]) and
176 APOA5 (OR=0.61, 95% CI [0.56-0.67]) had the most significant effects on AAA risk.
177 Seven of the 41 circulating proteins, including APOC3, APOA5, LPL, APOE, PLTP
178 (phospholipid transfer protein), PCSK9 (proprotein convertase subtilisin/kexin type 9),
179 and LPA (lipoprotein(A)), play an important role in lipid metabolism, especially in VLDL
180 and chylomicron metabolism (Fig 1B). Using multi-instrument variable (multi-IV) MR to
181 account for potential pleiotropy, six of the seven lipid metabolism-related proteins
182 (APOC3, LPL, APOE, PLTP, PCSK9, and LPA) were found to have causal effects on
183 AAA across inverse-variance weighted (IVW) MR, weighted median MR, and MR-Egger
184 analyses (Supplementary Table 2). Our previous GWAS findings demonstrated that 42
185 lead variants at the AAA risk loci are associated with major lipid fractions.[6] After
186 prioritizing the role of five major lipoprotein components (HDL-C, LDL-C, TG, APOA1,
187 and APOB) as risk factors for AAA, TG was the top-ranked independent risk factor for
188 AAA with a marginal inclusion probability of 0.81 (P=0.007; Supplementary Table 3).
189 Consistent with previous studies,[6-8] LDL-C, HDL-C, and APOA1 still were significant
190 factors (Supplementary Table 3). These genetic and proteomic findings indicate that TG-
191 related metabolism may play a substantial role in AAA pathogenesis.
192
193 To further identify genetic associations between circulating metabolic traits and AAA
194 risk, we utilized the data from a recently published GWAS study of 233 circulating
195 metabolites to perform a two-sample MR analysis.[20] The NMR-measured metabolites

196 included 213 lipid traits (lipids, lipoproteins, and fatty acids) and 20 non-lipid traits
197 (amino acids, ketone bodies, and glucose/glycolysis-related metabolites).[20] Lipoproteins
198 are classified by particle sizes (XXL, XL, L, M, S, and XS) and then subgrouped by the
199 components (particle number, phospholipids, cholesterol, cholesterol ester, free
200 cholesterol, and TG). For each metabolite, we used the IVW method as the primary MR
201 approach and MR-Egger analysis and weighted median-based regression methods as
202 sensitivity analyses. We demonstrated that TG-rich lipoproteins, including VLDL, IDL
203 (intermediate density lipoprotein), and LDL, and all the components in TRL particles,
204 were positively associated with AAA risk, while HDL and glucose were negatively
205 associated with AAA risk, consistent with population findings (Fig 1C, full MR results in
206 Supplementary Table 4).[9, 10, 21, 22] Interestingly, we noticed that the TG component in
207 HDL particles was positively associated with AAA risk compared to other components in
208 HDL particles, such as cholesterol and phospholipids (Fig 1C). Concomitantly, we
209 observed that total fatty acids and saturated fatty acids, the major metabolites of
210 triglycerides, were also positively associated with AAA risk. These findings raise the
211 possibility that lowering triglycerides and related metabolites could provide a therapeutic
212 pathway for reducing the risk of AAA.
213
214 **Impaired LPL activity accelerates AAA development and rupture.**
215 Chronic subcutaneous infusion of AngII serves as a well-established AAA model in
216 hypercholesterolemic mouse models, which includes using mice with deficiencies in
217 apolipoprotein E (*Apoe*) or LDL receptor (*Ldlr*) or manipulating by adeno-associated
218 virus-mediated overexpression of *Pcsk9* to induce hyperlipidemia.[23-25] Our previous
219 GWAS demonstrated that LPL variants that lead to increased plasma TG concentrations
220 were linked to an increased risk of AAA.[6] The MR analysis also identified circulating LPL
221 levels to be negatively associated with AAA risk (Fig 1B). To validate whether increased
222 TG concentrations caused by impaired LPL activity can result in AAA development and
223 rupture, we infused AngII into male, inducible *Lpl*-deficient (i*Lpl*$^{-/-}$) mice fed a low-
224 cholesterol Western diet. With AngII infusion, an aortic rupture occurred in 94% (16/17,
225 combined data from two independent studies) of i*Lpl*$^{-/-}$ mice compared to 9.5% (2/21,
226 combined data from two independent studies) aortic rupture rate in littermate control
227 mice (Fig 2A-C, Supplementary Fig 1). The only survival i*Lpl*$^{-/-}$ mouse did not have AAA
228 and had a plasma TG concentration of 474 mg/dL and TC concentration of 233 mg/dL.
229 In contrast, after 1 week of Western diet feeding but before AngII infusion, the majority
230 of the i*Lpl*$^{-/-}$ mice had severely increased TG concentrations, which were as high as
231 11,103 mg/dL (4,077 ± 3,218 mg/dL) compared to 66 ± 28 mg/dL in *Lpl*$^{f/f}$ mice
232 (Supplementary Fig 1A). Saline infusion, as a control, did not cause aortic rupture in
233 either genotype (Supplementary Fig 1C). These findings showed that severely

234 increased TG concentrations as a consequence of LPL deficiency resulted in aortic
235 rupture and death in the AngII-induced AAA model.
236
237 Then, we employed other mouse strains with increased, but not severely elevated, TG
238 concentrations to validate our hypothesis. We performed all the following AAA studies in
239 mice fed a standard rodent laboratory diet to minimize the effects of
240 hypercholesterolemia induced by a Western diet. ApoA-V is produced in the liver and
241 secreted into circulation, where it exerts an important role in regulating plasma TG
242 concentrations by enhancing LPL activity to hydrolyze triglycerides. Male *Apoa5*-
243 deficient mice showed a 2-3-fold increase in TG concentrations but no difference in TC
244 concentrations (Fig 2D-G, Supplementary Fig 2A-B), consistent with previous findings.[12]
245 Using size exclusion chromatography, we found increased TG concentrations in VLDL
246 and IDL (Supplementary Fig 2D-E) in the *Apoa5*-deficient mice compared to their
247 littermate WT controls, while cholesterol concentrations remained similar. Plasma non-
248 esterified fatty acids (NEFA), which are primarily released during TG hydrolysis, were
249 also significantly elevated in the *Apoa5*-deficient mice (Supplementary Fig 2C). AAA
250 was evaluated after a 4-week AngII infusion. The hypertriglyceridemic *Apoa5*-deficient
251 mice had increased AAA incidence and larger maximal abdominal aorta diameter (Fig
252 2E, H, I). Slightly increased TG concentrations in *Apoa5*-deficient mice promoted AAA
253 formation, but did not trigger aneurysm rupture and animal death. There was no
254 difference in blood pressure before and after AngII infusion between *Apoa5*-deficient
255 mice and their littermate controls (Fig 2J). This phenotype was not observed in *Apoa5*-
256 deficient female mice (Fig 2K-O), which had significantly lower TG concentrations
257 compared to male *Apoa5*-deficient mice (142 ± 51 mg/dL v.s. 327 ± 147 mg/dL, p =
258 0.003, Fig 2F and K). In addition, female mice demonstrate markedly lower incidences
259 of AAA than males due to sex hormones or sex chromosomes.[26] These findings imply
260 the causative roles of elevated TG concentrations in AAA pathogenesis.
261
262 **Moderately to severely increased triglyceride levels accelerate AAA development**
263 **and dissection in human *APOC3* transgenic mice.**
264 Increased plasma ApoC-III concentrations are linked to enhanced production and
265 slowed clearance of triglyceride-rich lipoproteins, causing hypertriglyceridemia. Human
266 *APOC3* transgenic (h*APOC3* Tg) mice and age/sex-matched wild-type littermates were
267 fed a standard rodent laboratory diet (Fig 3A). Compared with controls, male h*APOC3*
268 Tg mice had about 8-fold increase in plasma TG concentrations (Fig 3B) and about 1-
269 fold elevations in plasma TC concentrations (Fig 3C) and non-esterified fatty acids
270 (NEFA, Fig 3D). We observed a low incidence of AAA in wild-type littermates (2 out of
271 17), similar to the literature.[26] However, there was a dramatically increased AAA
272 incidence and a larger maximal diameter of the suprarenal aorta in h*APOC3* Tg mice

273 (11 out of 13 surviving animals), as well as a higher dissection rate (8 out of 13 surviving
274 animals) and another 2 mice dying from AAA rupture (Fig 3E-H, Supplementary Fig 11).
275 There was no difference in systolic blood pressure (SBP) between h*APOC3* Tg mice
276 and controls (Fig 3I). A similar phenotype was observed in female mice (Fig 3J-O),
277 which had 5-fold increase in TG concentrations compared to control mice, indicating
278 that dramatically increased TG concentrations accelerated AAA development,
279 surpassing the protective effects of female hormones.
280
281 The effects of increased TG concentrations on AAA development were also evaluated in
282 a PPE (porcine pancreatic elastase)-induced AAA model, in which AAA progression is
283 independent of hypercholesterolemia.[27] Based upon a 50% increase in the maximal
284 abdominal aorta diameter as AAA on day 14 post-operative, the incidence of AAA was
285 100% for both male and female h*APOC3* Tg and littermate control mice (Supplementary
286 Fig 3 and Supplementary Fig 4). Male h*APOC3* Tg mice showed significantly larger
287 maximal aortic diameters than littermate controls, demonstrating that increased TG
288 concentrations accelerated AAA growth (Supplementary Fig 3A-E). Even though female
289 h*APOC3* Tg mice had lower TG concentrations than males (635 ± 36 mg/dL v.s. 946 ±
290 258 mg/dL, $p = 0.0005$), the increased TG concentrations in females were sufficient to
291 cause larger aortic diameters (Supplementary Fig 4A-D).
292
293 These findings from the three hyperglyceridemia mouse models indicate that increased
294 TG concentrations accelerate AAA rupture and aneurysm growth.
295
296 **Palmitate and increased triglyceride concentrations inhibit lysyl oxidase**
297 **maturation in human aortic smooth muscle cells and aortas.**
298 The pathophysiology of AAA is intricately linked to the disruption of smooth muscle cell
299 (SMC) homeostasis within the aortic wall, including phenotypic switching, cell death,
300 extracellular matrix (ECM) remodeling, and inflammatory responses.[28] Serum from
301 *Apoa5*-deficient or h*APOC3* Tg mice, as well as VLDL and HDL particles, did not affect
302 primary human aortic smooth muscle cell (HASMC) viability (Supplementary Fig 5)).
303 Overexpression of APOC3 in h*APOC3* transgenic mice caused elevated plasma TG
304 concentrations accompanied by increased plasma NEFA concentrations (Fig 3D and
305 Supplementary Fig 3C). The high availability of fatty acids in the liver further increases
306 triglyceride synthesis, resulting in VLDL assembly and secretion. Using MR, we
307 confirmed the causal association between genetically determining plasma TG level and
308 circulating total fatty acid concentrations (Fig 4A). Palmitic acid (PA, 16:0), stearic acid
309 (18:0), palmitoleic acid (16:1n-7), and oleic acid (18:1n-9) are major saturated and
310 monounsaturated fatty acids that affect cellular signaling and metabolic pathways.[29] PA
311 is the most common saturated fatty acid in the human body, typically accounting for 20–

312 30% of the total fatty acids.[30] MR analysis found that increased TG causally increased
313 PA level, but not the other three fatty acids (Fig 4A), suggesting PA serves as an
314 important metabolite in mediating the AAA-promoting effects of high TG or high TG-
315 related mutations. Using untargeted metabolomics, we found elevated plasma ethyl
316 palmitate levels (a lipid-soluble form of PA) in h*APOC3* Tg mice (Fig 4B). Bulk RNA
317 sequencing (RNA-seq) analysis was performed to compare PA-incubated HASMC with
318 BSA-treated (vehicle control) cells. Compared to the BSA-incubated group, PA-
319 incubated HASMC showed an apparent reduction in ECM assembly pathways,
320 including collagen chain trimerization, elastic fiber formation and maturation (Fig 4C-E),
321 and increased expression of the inflammation-related gene (Supplementary Fig 6A-B,
322 Supplementary Table 5).
323
324 TGF-β and lysyl oxidase (LOX) are crucial in regulating the cross-linking of collagen and
325 elastin in the ECM. LOX was unexpectedly upregulated compared to the most
326 downregulated genes in the elastic fiber formation and maturation pathways (Fig 4E). In
327 primary HASMC, PA incubation induced the transcription of LOX, showing increased
328 mRNA abundance by qRT-PCR (Fig 4F). LOX is initially synthesized as a preproprotein,
329 which undergoes several post-translational modifications for its maturation and
330 functional activation. Impairments in LOX activity, whether due to genetic mutations or
331 LOX inhibitors, can lead to AAA formation and rupture.[31-33] Our RNA-seq data indicated
332 that PA incubation downregulated the expression of BMP-1 (Bone morphogenetic
333 protein 1), ADAMTS2 (a disintegrin and metalloproteinase with thrombospondin motif 2),
334 and ADAMTS14, which are critical enzymes controlling LOX activation by the proteolytic
335 removal of the propeptide region.[34] We further confirmed that PA incubation
336 downregulated BMP-1 and ADAMTS2 transcriptions in HASMC (Fig 4G, Supplementary
337 Fig 7A). Immunoblot analyses demonstrated that incubation with TGF-β increased the
338 abundance of the mature form of LOX both in the conditioned medium and cell lysates
339 of HASMC. However, the presence of PA blocked its effect, resulting in a less mature
340 LOX (Fig 4I, J, Supplementary Fig 7H). LOX overexpression increased the mature form
341 of LOX in HASMC, which was suppressed by incubation with PA (Fig 4I,J,
342 Supplementary Fig 7I), indicating that PA interferes with the maturation process of LOX
343 in HASMC.
344
345 To investigate how PA influences LOX maturation, using siRNA-mediated gene silence
346 of *BMP1*, *ADAMTS2*, or *ADAMTS14* in HASMC, we found that *BMP1* knockdown led to
347 dramatically decreased LOX maturation in the conditioned medium (Supplementary Fig
348 7E-F), suggesting that BMP-1 is the primary enzyme regulating LOX maturation in
349 HASMC. Additionally, *BMP1* knockdown increased LOX transcription (Supplementary
350 Fig 7G), likely as a compensatory effect; however, it was insufficient to compensate for

351 the loss of mature LOX. Next, we investigated whether LOX overexpression can restore
352 mature LOX levels within the PA-BMP-1 axis. In the presence of PA or knockdown of
353 *BMP1*, LOX maturation was largely impaired (Figure 4I and L), showing dramatically
354 reduced mature bands. Overexpression of LOX restored mature LOX levels (Figure 4I
355 and L), suggesting that LOX overexpression may prevent the pro-AAA effects of high
356 TG and PA levels. Our previous study validated the utility of tissue-crosstalk analysis for
357 investigating organ-organ interactions.[35] Among the >1,800 secreted proteins in the
358 liver, APOC3 ranked 52nd in terms of its impact on aortic gene expression. Among the
359 131 donors from the GTEx project, liver *APOC3* RNA expression showed a strong
360 negative association with *BMP1* RNA expression in the aorta (Fig 4H), whereas the
361 associations with *ADAMTS2* and *ADAMTS14* were much weaker (Supplementary Fig
362 7B-C). In contrast, liver *APOC3* expression was positively associated with aortic *LOX*
363 expression (Supplementary Fig 7D). The tissue-crosstalk analysis suggests that liver-
364 secreted APOC3 regulates aortic gene expression, including BMP1 and LOX, essential
365 for vascular integrity, potentially influencing aortic extracellular matrix remodeling and
366 contributing to AAA pathogenesis.
367
368 To investigate the effects of increased circulating palmitate concentrations on the
369 maturation of LOX in aortas, we administered ethyl palmitate, which can be hydrolyzed
370 to free palmitate in rodents.[36] The mature LOX abundance in suprarenal abdominal
371 aortas was decreased significantly after administration of ethyl palmitate compared to
372 the vehicle or saline control aortas (Fig 4M). Then, we examined whether increased TG
373 concentrations affected the maturation of LOX in the aortas of h*APOC3* Tg and
374 littermate control mice. There was no difference in the abundance of mature LOX in
375 suprarenal abdominal aortas between the two groups without AngII infusion (Fig 4N).
376 We observed a dramatic upregulation of mature LOX upon AngII infusion in control mice
377 (Fig 4N), suggesting a protective and compensatory mechanism to enhance elastic fiber
378 assembly to protect against the effects of AngII. However, this response was absent in
379 h*APOC3* Tg mice (Fig 4N), indicating that increased TG and/or palmitate inhibited LOX
380 maturation in the aortas, which may contribute to AAA development and rupture.
381
382 **LOX overexpression effectively prevents AAA formation and dissection in**
383 **h*APOC3* Tg Mice**
384 These findings suggest that TG and palmitate promote AAA development by disrupting
385 essential LOX maturation. To validate this mechanism *in vivo*, we utilized an adenoviral
386 vector to overexpress LOX in the suprarenal abdominal aorta of both WT and h*APOC3*
387 Tg mice, followed by an 18-day AngII infusion (Fig 5A). First, we confirmed that local
388 adenovirus application successfully increased the expression of LOX or GFP (as
389 control) in the target region (Supplementary Fig 8). LOX overexpression (LOX OE) did

390 not affect the rupture rate (Supplementary Fig 11) or induce AAA formation in WT mice
391 (Fig 5B-E). Strikingly, none of the h*APOC3* Tg mice developed AAA when LOX was
392 overexpressed locally alongside AngII induction, compared to a 67% AAA incidence and
393 a 44% dissection rate in the GFP-overexpressed control group (Fig 5B-D). LOX OE
394 significantly reduced the maximal suprarenal abdominal aorta diameter (Fig 5E), without
395 affecting SBP (Fig 5F), body weight (Fig 5G), TG (Fig 5H), TC (Fig 5I), and NEFA levels
396 (Fig 5J). Histological analysis revealed that h*APOC3* Tg mice exhibited substantial
397 collagen disorganization and elastic fiber degradation compared to WT mice, indicating
398 impaired LOX function (Fig 5K). Notably, LOX OE restored these structural features and
399 reinforced vascular wall integrity, even in the presence of elevated TG levels (Fig 5K).
400 Taken together, these results established that impaired LOX activation is a key
401 mechanism by which elevated TG levels contribute to AAA development.
402
403 ***Angptl3* ASO inhibits AAA formation and dissection in *APOC3* Tg mice.**
404 Based on the above findings, we asked whether lowering TG levels could attenuate
405 AAA formation and dissection. We administrated fenofibrate and niacin, commonly used
406 for treating hypertriglyceridemia, but only observed a 14-17 % reduction of plasma TG
407 concentrations in h*APOC3* Tg mice (Supplementary Fig 9). N-acetylgalactosamine
408 (GalNAc)-conjugated antisense nucleotides (ASO) targeting of hepatocyte ANGPTL3
409 results in significantly decreased plasma TG concentrations in animals and humans.[15,
410 16, 37] In h*APOC3* Tg mice, administration of *Angptl3* ASO dramatically suppressed
411 hepatic *Angptl3* mRNA abundance by 64% and the plasma ANGPTL3 concentrations by
412 81% (Fig 6A-C). Consequently, administration of the *Angptl3* ASO significantly reduced
413 concentrations of NEFA, triglycerides (from 1,119 ± 98 mg/dL to 586 ± 114 mg/dL) and
414 total cholesterol (from 283 ± 103 mg/dL to 117 ± 58 mg/dL) (Fig 6D-F). Consistent with
415 the above findings, increased TG concentrations in h*APOC3* Tg mice accelerated AAA
416 development during AngII infusion (Fig 6G-L). After administration of *Angptl3* ASO to
417 h*APOC3* Tg mice, we recorded significant reductions in AAA incidence, maximal aortic
418 diameter, elastin degradation, and dissection, comparable to the control mice (Fig 6G-
419 L). qRT-PCR and ELISA analysis showed no significant changes in the levels of mouse
420 *Apoc3* and human *APOC3* (Fig 6M-P). There were no significant changes in the TG and
421 TC metabolism-related genes in the liver, such as *Apoc2*, *Apoa5*, *Apoe*, *Apob*, *Mttp*,
422 *Fasn*, *Srebp1c*, *Ldlr*, and *Pcsk9* (Supplementary Fig 10). *Angptl3* ASO administration
423 did not significantly change body weight or systolic blood pressure (Fig 6Q-R). Overall,
424 our findings demonstrate that administration of *Angptl3* ASO protected against
425 hypertriglyceridemia accelerated AAA development in h*APOC3* Tg mice.
426
427 ***Angptl3* ASO inhibits AAA development in *Apoe*-deficient mice.**

428 ApoE-deficient mice have high levels of VLDL due to impaired clearance of chylomicron
429 and VLDL. Compared with age and sex-matched C57BL/6J mice, *Apoe*-deficient mice
430 show significantly increased plasma levels of TC and moderately increased TG levels
431 when fed a standard rodent diet.[38] Similar to the observation in h*APOC3* Tg mice,
432 administration of *Angptl3* ASO dramatically reduced hepatic *Angptl3* mRNA expression
433 and the circulating levels of ANGPTL3 (Fig 7A-C). As expected, administration of the
434 *Angptl3* ASO significantly decreased TG concentrations by 50%, NEFA by 31%, and
435 slightly decreased TC concentrations by 8% in *Apoe*-deficient mice fed a standard
436 rodent laboratory diet (Fig 7D-F). We also used size exclusion chromatography to
437 separate lipoprotein classes and found decreased TG concentrations, mainly in VLDL
438 and IDL (Fig 7I), while cholesterol concentrations were slightly reduced in VLDL and
439 HDL (Fig 7J). Blood pressure measurements and body weight recordings revealed no
440 significant difference between control ASO and *Angptl3* ASO-administered mice (Fig
441 7G, H). Consistent with the literature, AAA incidence in *Apoe*-deficient mice was 83% in
442 the control group (Fig 7K, N). *Angptl3* ASO administration largely inhibited AAA
443 development, as evidenced by significantly decreased AAA incidence and maximal
444 aortic diameters (Fig 7N, O). Depletion of hepatic *Angptl3* had limited effects on the
445 expression of genes involved in lipogenesis and cholesterol metabolism (Fig 7P). Taken
446 together, these data demonstrated that lowering TG and NEFA concentrations by
447 *Angptl3* ASO inhibited AAA development in *Apoe*-deficient mice.
448
449 **Discussion**

450 AAA screening programs have identified many asymptomatic AAA and effectively
451 reduced aneurysm-related mortality. Thus, limiting aneurysm growth and reducing the
452 risk of aneurysm rupture has become a key priority for the treatment of AAA.[39] Based on
453 the genetic, proteomic, and metabolomic findings, we identify that increased TG
454 concentrations accelerate AAA formation, dissection, and rupture using three
455 hypertriglyceridemic mouse models. Of clinical relevance, we provide evidence that
456 lowering TG and NEFA concentrations by *Angptl3* ASO administration dramatically
457 inhibited AAA development and dissection.
458
459 Mendelian Randomization (MR) using protein quantitative trait loci (pQTLs) as
460 instrumental variables (IVs) can help infer causality and identify drug targets for
461 complex diseases. By integrating pQTLs from ten large GWAS on circulating proteins,
462 we updated the 'actionable' druggable target pool into an enlarged set of 2,698 proteins.
463 Genetically determined APOA5 and LPL, two critical molecules regulating triglyceride
464 metabolism, were negatively associated with AAA risk. In contrast, the variants related
465 to APOC3 with increased TG concentrations were associated with increased AAA risk,

underscoring the role of triglyceride metabolism in human AAA development, consistent with other genetic findings.[7, 8] We further explored the causal effects of metabolites on AAA risk using IVs from 233 NMR-measured circulating metabolites.[20] The strong associations found in VLDL and its subfractions as well as free fatty acid concentrations, further highlighted the importance of TG metabolism in AAA. Collectively, these findings emphasize the significance of TG in AAA risk and provide potential candidates for AAA prevention and treatment.

According to the literature and our experience, young C57BL/6J mice, when fed a standard rodent laboratory diet, have low AAA incidence when infused with AngII.[26, 40] Hyperlipidemia increases the AAA incidence during AngII infusion in *Ldlr* and *Apoe*-deficient mice or C57BL/6J mice with an AAV expressing a gain-of-function mutant of PCSK9, in which *Ldlr*-deficient mice and PCSK9 overexpressing mice are fed a Western diet to augment hypercholesterolemia.[26] Compared with C57BL/6J mice, *Ldlr* or *Apoe*-deficient mice have significantly increased TC and TG concentrations, which mainly distribute in VLDL fractions using size exclusion chromatography to separate lipoprotein classes,[41] indicating that increased concentrations of large, TG-rich lipoproteins are associated with AAA formation. Our previous study demonstrated that AAA development is accelerated with modestly hypercholesterolemic conditions, but further elevation of cholesterol above a threshold level does not enhance AAA progression.[40] Here, we present that increased TG concentrations contribute to AAA development, dissection, and rupture in a TG-concentration-dependent manner (Supplementary Table 7) using three hypertriglyceridemia mouse models. The moderately increased TG concentrations in *Apoa5* deficiency mice accelerated AAA development, dramatically increased TG concentrations in h*APOC3* transgenic mice caused AAA dissection, and severely high TG concentrations resulted in aortic rupture and death in inducible *Lpl*-deficient mice. We also evaluated the effects of increased TG concentrations on aneurysm growth in the elastase-induced AAA model. Previous studies have demonstrated that the aneurysm growth in the PPE model is independent of hypercholesterolemic conditions using C57BL/6J mice with PCSK9 overexpression or *Apoe*-deficient mice.[27, 42] Using the PPE-induced AAA model, we demonstrated that increased TG concentrations aggravated AAA growth in both male and female h*APOC3* Tg mice. Furthermore, clinical observation shows that plasma TG concentrations are higher in AAA patients than in controls.[9] In a prospective epidemiological study (the British United Provident Association [BUPA] study), the risk of death from AAA rupture is strongly related to serum TG concentrations.[10] Together, these findings pave the way for future studies of the role of triglyceride and related metabolites in AAA development.

Importantly, our study demonstrates that lowering TG and NEFA levels by administrating *Angptl3* ASO inhibits AAA development in both h*APOC3* transgenic mice and *Apoe*-deficient mice. ApoC-III raises TG concentrations by inhibiting LPL activity, reducing hepatic uptake of TG-rich lipoproteins, and promoting VLDL secretion. ApoE acts as a critical ligand for the LDL receptor and the LDL receptor-related protein, facilitating the uptake of chylomicron and VLDL remnants into hepatocytes. Deficiency of ApoE causes elevated TG and TC levels. In both *APOC3* transgenic mice and *Apoe*-deficient mice, triglycerides and cholesterol are mainly distributed in VLDL fractions. Administration of *Angptl3* ASO dramatically reduced TG levels in VLDL and IDL fractions, consistent with decreased TG concentrations in plasma, supporting the hypothesis that large-sized TG-rich lipoproteins and related metabolites contribute to AAA progression and rupture. These findings also provide evidence that lowering TG-rich lipoproteins is a potential therapeutic strategy. ANGPTL8 and ANGPTL3 form a complex that markedly inhibits LPL activity. Similar to the effects of *Angptl3* ASO on AAA, *Angplt8*-deficiency or knockdown reduced AAA formation by lowering TG concentrations and suppressing the inflammatory response in *Apoe*-deficient mice.[43] Administration of fenofibrate also reduced the severity of experimental AAA in *Ldlr*- and *Apoe*-deficient mice.[44, 45] However, fenofibrate did not significantly limit AAA growth in AAA patients in FAME-2 (Fenofibrate in the Management of Abdominal Aortic Aneurysm 2), a placebo-controlled clinical trial.[46] We should note that it may take an estimated five years for a small AAA with a diameter of 40–55 mm to reach 55 mm, the size threshold for intervention.[39] In the FAME-2 study, AAA diameters in the control group increased only about 1 mm after a 24-week observation period, making it hard to determine the effects of fenofibrate. Additionally, AAA diameters in the two groups began to diverge at the end of the evaluation, suggesting that a long-term clinical trial with a larger sample size is needed to carefully assess the effects of triglyceride-lowering on AAA growth and rupture. Statins primarily target TC but also have a moderate TG-lowering effect (10–30%), depending on the statin type and dose. While observational studies have found potential benefits of statins in AAA management by reducing inflammation, stabilizing the aortic wall, and lowering TC and TG levels, their impact on AAA growth and rupture risk remains controversial and inconclusive[47-49]. This variability may be influenced by differences in statin types, dosages, and genetic metabolic-related factors. Therefore, high-quality randomized controlled trials are needed further to clarify their role in AAA prevention and treatment.

AAA is characterized by pathological remodeling of the aortic ECM, including elastolysis and collagenolysis. LOX is a crucial enzyme involved in the cross-linking of collagen and elastin in the ECM to maintain the structural integrity of the aortic wall. Impairments in LOX activity due to genetic mutations can lead to connective tissue disorders and

543 promote aorta dissection.[50] *Lox*-deficient mice exhibit severe defects in vascular
544 development, leading to perinatal death from aortic aneurysm.[32] β-Aminopropionitrile
545 (BAPN) is a well-known inhibitor of LOX and has been used extensively in research to
546 accelerate AAA formation and rupture.[51] LOX is initially synthesized as a preproprotein
547 and secreted into the extracellular space, where the prolysyl oxidase is cleaved by
548 proteases, including BMP-1, ADAMTS-2, and ADAMTS-14. Increased TG
549 concentrations or the presence of palmitate dramatically blocked LOX maturation in
550 aortas and HASMC. Based on RNA-seq findings, *BMP1* and *ADAMTS2* are highly
551 abundant in HASMC. PA downregulated the expression of *BMP1* and *ADAMTS2*,
552 causing decreased LOX maturation. In this study, we confirmed BMP-1 is the
553 predominant enzyme regulating LOX maturation in HASMC. The increase in LOX
554 transcription upon *BMP1* knockdown or palmitate treatment was likely a compensatory
555 response; however, it was insufficient to compensate for the loss of mature LOX.
556 Increasing the substrate availability through LOX overexpression could partially
557 compensate for reduced BMP-1 function and produce a certain amount of mature LOX.
558 Further analysis of liver-aorta crosstalk using data from the GTEx project revealed that
559 the liver is predicted to influence aortic gene expression through the secretion of
560 APOC3. Notably, higher liver *APOC3* levels are associated with lower *BMP1* expression
561 in the aorta. Previous studies have shown that LOX overexpression can inhibit AAA
562 development in the $CaCl_2$-induced AAA model.[52] In our AngII model in h*APOC3* Tg
563 mice, local LOX overexpression in the suprarenal aorta completely abolished the effects
564 of high TG on promoting suprarenal AAA. Additionally, PA induces vascular SMC
565 apoptosis, promotes inflammatory responses, enhances oxidative stress, and triggers
566 proliferation and migration, contributing to the progression of vascular diseases such as
567 atherosclerosis and hypertension.[53] In this study, we demonstrated that PA, as a
568 metabolite of plasma triglycerides or endogenously synthesized in the liver, may
569 contribute to AAA development by inhibiting LOX maturation. These findings uncover a
570 novel liver-aorta regulatory mechanism where APOC3-induced hypertriglyceridemia
571 suppresses BMP-1 and impairs LOX maturation, potentially driving AAA formation.
572
573 Plasma TG concentrations include the content of various lipoprotein particles. Multiple
574 genes, such as LPL, APOC3, APOC2, APOA5, and ANGPTL3, influence TG
575 metabolism and regulate plasma TG concentrations. Among them, APOC3 and
576 ANGPTL3 are targets for drug development because loss-of-function mutations in
577 APOC3 and ANGPTL3 are associated with improved lipid profiles and reduced
578 cardiovascular risk. Preclinical and clinical data have well documented that ApoC-III or
579 ANGPTL3 inhibitors effectively reduce severe hypertriglyceridemia. These inhibitors
580 include antisense nucleotides (ASO),[14, 16, 37] monoclonal antibodies (mAb),[54] small
581 interfering RNA (siRNA),[55, 56], and CRISPR-cas gene editing strategies.[57, 58] Preclinical

582 and clinical data have demonstrated that ANGPTL3 inhibitors are highly effective for
583 treating severe hypertriglyceridemia by upregulating LPL activity and facilitating the
584 hydrolysis and clearance of TG-rich lipoproteins. As h*APOC3* transgenic mice have very
585 high APOC3 and TG concentrations, *Angptl3* ASO was administrated at 50 mg/kg/week
586 in previous studies.[16] In this study, administration of an *Angptl3* ASO at a much lower
587 dosage effectively reduced AAA development in h*APOC3* transgenic mice and *Apoe*-
588 deficient mice through reducing TG concentrations, especially TG concentrations in
589 VLDL fractions. We observed that the administration of *Angptl3* ASO mainly decreased
590 plasma TG concentrations with a limited reduction in plasma TC concentrations, further
591 supporting the idea that managing TG-rich lipoprotein concentrations is a potential
592 therapeutic strategy for treating AAA.
593
594 This study has several limitations. First, while our animal models exhibit increased TG
595 levels, some also show concurrent alterations in TC levels, making it challenging to fully
596 distinguish their independent effects. However, the strong correlation between TG levels
597 and AAA severity, the mechanistic link between TG and LOX inhibition, and the
598 therapeutic efficacy of TG-lowering strategies via *Angptl3* ASO administration
599 collectively support a direct role of hypertriglyceridemia in AAA pathogenesis. Second,
600 although the *Lpl*-KO mouse model provides valuable insights into the impact of severe
601 TG elevation on AAA, its extreme hypertriglyceridemia limits translational relevance. To
602 address this, we incorporated moderate hypertriglyceridemia models for mechanistic
603 and therapeutic studies. *Lpl*-KO mice exhibit severely elevated TG and chylomicron
604 levels, closely mirroring human familial chylomicronemia syndrome, a rare and severe
605 condition affecting approximately 1 in 1,000,000 individuals[59]. In contrast, heterozygous
606 h*APOC3*-Tg, *ApoA5*-deficient, and *ApoE*-deficient mice develop mild to moderate
607 hypertriglyceridemia when fed a standard chow diet, resembling familial
608 hypertriglyceridemia, a more common disorder affecting approximately 1 in 100
609 individuals.[60] Future studies utilizing animal models with selective modulation of TG,
610 cholesterol, or TG-rich lipoprotein levels will be essential to clarify further their distinct
611 contributions to AAA pathogenesis and therapeutic targeting.
612
613 In summary, the present studies, combined with recent genetic, proteomic, and
614 metabolomic findings, indicate that increased TG concentrations contribute to an
615 increased risk of AAA. Individuals with higher genetic predisposition for AAA may benefit
616 from targeted interventions. Understanding the association between triglyceride
617 concentrations and AAA risk has important clinical implications. Notably, our results
618 demonstrate that ASO therapy targeting liver ANGPTL3 holds potential as a therapeutic
619 approach to reduce AAA risk. These findings underscore the need for additional

experimental and clinical investigations into the mechanisms and therapeutic strategies for AAA treatment through triglyceride-lowering therapies.

Funding

This study was partially supported by the National Institutes of Health grants HL166203 (Y.G.), HL165688 (Y.G. and A.S.), HL109946 and HL134569 (Y.E.C.), HL151524 (L.C.), HL153710 and HL138139 (J.Z.), HL172832 (G. Zhao), R35HL155649 (A.D.), UL1TR001998 (A.D.), R21 NS11191 (A.S.) and the American Heart Association Merit award 23MERIT1036341 (A.D.).

Disclosures

The authors have no competing interests.

Data availability

All genetic data used in this study were obtained from publicly available consortiums. The RNAseq original data generated during this study will be deposited in a publicly accessible database upon acceptance of the manuscript.

637 **References**

638 1. Nordon IM, Hinchliffe RJ, Loftus IM and Thompson MM. Pathophysiology and
639 epidemiology of abdominal aortic aneurysms. *Nat Rev Cardiol*. 2011;8:92-102.
640 2. United Kingdom Small Aneurysm Trial P, Powell JT, Brady AR, Brown LC,
641 Fowkes FG, Greenhalgh RM, Ruckley CV and Thompson SG. Long-term outcomes of
642 immediate repair compared with surveillance of small abdominal aortic aneurysms. *N*
643 *Engl J Med*. 2002;346:1445-52.
644 3. Soden PA, Zettervall SL, Ultee KH, Darling JD, Buck DB, Hile CN, Hamdan AD
645 and Schermerhorn ML. Outcomes for symptomatic abdominal aortic aneurysms in the
646 American College of Surgeons National Surgical Quality Improvement Program. *J Vasc*
647 *Surg*. 2016;64:297-305.
648 4. Reimerink JJ, van der Laan MJ, Koelemay MJ, Balm R and Legemate DA.
649 Systematic review and meta-analysis of population-based mortality from ruptured
650 abdominal aortic aneurysm. *Br J Surg*. 2013;100:1405-13.
651 5. Golledge J, Thanigaimani S, Powell JT and Tsao PS. Pathogenesis and
652 management of abdominal aortic aneurysm. *Eur Heart J*. 2023;44:2682-2697.
653 6. Roychowdhury T, Klarin D, Levin MG, Spin JM, Rhee YH, Deng A, Headley CA,
654 Tsao NL, Gellatly C, Zuber V, et al. Genome-wide association meta-analysis identifies
655 risk loci for abdominal aortic aneurysm and highlights PCSK9 as a therapeutic target.
656 *Nat Genet*. 2023;55:1831-1842.
657 7. Harrison SC, Holmes MV, Burgess S, Asselbergs FW, Jones GT, Baas AF, van 't
658 Hof FN, de Bakker PIW, Blankensteijn JD, Powell JT, et al. Genetic Association of Lipids
659 and Lipid Drug Targets With Abdominal Aortic Aneurysm: A Meta-analysis. *JAMA*
660 *Cardiol*. 2018;3:26-33.
661 8. Klarin D, Damrauer SM, Cho K, Sun YV, Teslovich TM, Honerlaw J, Gagnon DR,
662 DuVall SL, Li J, Peloso GM, et al. Genetics of blood lipids among ~300,000 multi-ethnic
663 participants of the Million Veteran Program. *Nat Genet*. 2018;50:1514-1523.
664 9. Norrgard O, Angquist KA and Johnson O. Familial aortic aneurysms: serum
665 concentrations of triglyceride, cholesterol, HDL-cholesterol and (VLDL + LDL)-
666 cholesterol. *Br J Surg*. 1985;72:113-6.
667 10. Watt HC, Law MR, Wald NJ, Craig WY, Ledue TB and Haddow JE. Serum
668 triglyceride: a possible risk factor for ruptured abdominal aortic aneurysm. *Int J*
669 *Epidemiol*. 1998;27:949-52.
670 11. Subramanian S. Hypertriglyceridemia: Pathophysiology, Role of Genetics,
671 Consequences, and Treatment. In: K. R. Feingold, B. Anawalt, M. R. Blackman, A.
672 Boyce, G. Chrousos, E. Corpas, W. W. de Herder, K. Dhatariya, K. Dungan, J. Hofland,
673 S. Kalra, G. Kaltsas, N. Kapoor, C. Koch, P. Kopp, M. Korbonits, C. S. Kovacs, W.
674 Kuohung, B. Laferrere, M. Levy, E. A. McGee, R. McLachlan, M. New, J. Purnell, R.

675 Sahay, A. S. Shah, F. Singer, M. A. Sperling, C. A. Stratakis, D. L. Trence and D. P.
676 Wilson, eds. *Endotext* South Dartmouth (MA); 2000.
677 12. Pennacchio LA, Olivier M, Hubacek JA, Cohen JC, Cox DR, Fruchart JC, Krauss
678 RM and Rubin EM. An apolipoprotein influencing triglycerides in humans and mice
679 revealed by comparative sequencing. *Science*. 2001;294:169-73.
680 13. Breckenridge WC, Little JA, Steiner G, Chow A and Poapst M.
681 Hypertriglyceridemia associated with deficiency of apolipoprotein C-II. *N Engl J Med*.
682 1978;298:1265-73.
683 14. Witztum JL, Gaudet D, Freedman SD, Alexander VJ, Digenio A, Williams KR,
684 Yang Q, Hughes SG, Geary RS, Arca M, et al. Volanesorsen and Triglyceride Levels in
685 Familial Chylomicronemia Syndrome. *N Engl J Med*. 2019;381:531-542.
686 15. Bergmark BA, Marston NA, Prohaska TA, Alexander VJ, Zimerman A, Moura FA,
687 Murphy SA, Goodrich EL, Zhang S, Gaudet D, et al. Olezarsen for Hypertriglyceridemia
688 in Patients at High Cardiovascular Risk. *N Engl J Med*. 2024;390:1770-1780.
689 16. Graham MJ, Lee RG, Brandt TA, Tai LJ, Fu W, Peralta R, Yu R, Hurh E, Paz E,
690 McEvoy BW, et al. Cardiovascular and Metabolic Effects of ANGPTL3 Antisense
691 Oligonucleotides. *N Engl J Med*. 2017;377:222-232.
692 17. Rosenson RS, Gaudet D, Hegele RA, Ballantyne CM, Nicholls SJ, Lucas KJ, San
693 Martin J, Zhou R, Muhsin M, Chang T, et al. Zodasiran, an RNAi Therapeutic Targeting
694 ANGPTL3, for Mixed Hyperlipidemia. *N Engl J Med*. 2024.
695 18. Burgess S, Mason AM, Grant AJ, Slob EAW, Gkatzionis A, Zuber V, Patel A, Tian
696 H, Liu C, Haynes WG, et al. Using genetic association data to guide drug discovery and
697 development: Review of methods and applications. *Am J Hum Genet*. 2023;110:195-
698 214.
699 19. Gaziano L, Giambartolomei C, Pereira AC, Gaulton A, Posner DC, Swanson SA,
700 Ho YL, Iyengar SK, Kosik NM, Vujkovic M, et al. Actionable druggable genome-wide
701 Mendelian randomization identifies repurposing opportunities for COVID-19. *Nat Med*.
702 2021;27:668-676.
703 20. Karjalainen MK, Karthikeyan S, Oliver-Williams C, Sliz E, Allara E, Fung WT,
704 Surendran P, Zhang W, Jousilahti P, Kristiansson K, et al. Genome-wide
705 characterization of circulating metabolic biomarkers. *Nature*. 2024;628:130-138.
706 21. Ibrahim M, Thanigaimani S, Singh TP, Morris D and Golledge J. Systematic
707 review and Meta-Analysis of Mendelian randomisation analyses of Abdominal aortic
708 aneurysms. *Int J Cardiol Heart Vasc*. 2021;35:100836.
709 22. Raffort J, Lareyre F, Clement M, Hassen-Khodja R, Chinetti G and Mallat Z.
710 Diabetes and aortic aneurysm: current state of the art. *Cardiovasc Res*. 2018;114:1702-
711 1713.

712 23. Daugherty A and Cassis L. Chronic angiotensin II infusion promotes
713 atherogenesis in low density lipoprotein receptor -/- mice. *Ann N Y Acad Sci*.
714 1999;892:108-18.
715 24. Daugherty A, Manning MW and Cassis LA. Angiotensin II promotes
716 atherosclerotic lesions and aneurysms in apolipoprotein E-deficient mice. *J Clin Invest*.
717 2000;105:1605-12.
718 25. Lu H, Howatt DA, Balakrishnan A, Graham MJ, Mullick AE and Daugherty A.
719 Hypercholesterolemia Induced by a PCSK9 Gain-of-Function Mutation Augments
720 Angiotensin II-Induced Abdominal Aortic Aneurysms in C57BL/6 Mice-Brief Report.
721 *Arterioscler Thromb Vasc Biol*. 2016;36:1753-7.
722 26. Sawada H, Lu HS, Cassis LA and Daugherty A. Twenty Years of Studying AngII
723 (Angiotensin II)-Induced Abdominal Aortic Pathologies in Mice: Continuing Questions
724 and Challenges to Provide Insight Into the Human Disease. *Arterioscler Thromb Vasc*
725 *Biol*. 2022;42:277-288.
726 27. Mulorz J, Spin JM, Beck HC, Tha Thi ML, Wagenhauser MU, Rasmussen LM,
727 Lindholt JS, Tsao PSC and Steffensen LB. Hyperlipidemia does not affect development
728 of elastase-induced abdominal aortic aneurysm in mice. *Atherosclerosis*. 2020;311:73-
729 83.
730 28. Golledge J. Abdominal aortic aneurysm: update on pathogenesis and medical
731 treatments. *Nat Rev Cardiol*. 2019;16:225-242.
732 29. Wu JH, Lemaitre RN, Manichaikul A, Guan W, Tanaka T, Foy M, Kabagambe EK,
733 Djousse L, Siscovick D, Fretts AM, et al. Genome-wide association study identifies
734 novel loci associated with concentrations of four plasma phospholipid fatty acids in the
735 de novo lipogenesis pathway: results from the Cohorts for Heart and Aging Research in
736 Genomic Epidemiology (CHARGE) consortium. *Circ Cardiovasc Genet*. 2013;6:171-83.
737 30. Carta G, Murru E, Banni S and Manca C. Palmitic Acid: Physiological Role,
738 Metabolism and Nutritional Implications. *Front Physiol*. 2017;8:902.
739 31. Staiculescu MC, Kim J, Mecham RP and Wagenseil JE. Mechanical behavior
740 and matrisome gene expression in the aneurysm-prone thoracic aorta of newborn lysyl
741 oxidase knockout mice. *Am J Physiol Heart Circ Physiol*. 2017;313:H446-H456.
742 32. Lee VS, Halabi CM, Hoffman EP, Carmichael N, Leshchiner I, Lian CG, Bierhals
743 AJ, Vuzman D, Brigham Genomic M, Mecham RP, et al. Loss of function mutation in
744 LOX causes thoracic aortic aneurysm and dissection in humans. *Proc Natl Acad Sci U S*
745 *A*. 2016;113:8759-64.
746 33. Franklin MK, Sawada H, Ito S, Howatt DA, Amioka N, Liang CL, Zhang N, Graf
747 DB, Moorleghen JJ, Katsumata Y, et al. beta-Aminopropionitrile Induces Distinct
748 Pathologies in the Ascending and Descending Thoracic Aortic Regions of Mice.
749 *Arterioscler Thromb Vasc Biol*. 2024;44:1555-1569.

750 34. Rosell-García T, Paradela A, Bravo G, Dupont L, Bekhouche M, Colige A and
751 Rodriguez-Pascual F. Differential cleavage of lysyl oxidase by the metalloproteinases
752 BMP1 and ADAMTS2/14 regulates collagen binding through a tyrosine sulfate domain.
753 *J Biol Chem*. 2019;294:11087-11100.
754 35. Liu Y, Yu M, Wang H, Dorsey KH, Cheng Y, Zhao Y, Luo Y, Zhao G, Zhao Y, Lu H,
755 et al. Restoring Vascular Smooth Muscle Cell Mitochondrial Function Attenuates
756 Abdominal Aortic Aneurysm in Mice. *Arterioscler Thromb Vasc Biol*. 2025.
757 36. Eguchi K, Manabe I, Oishi-Tanaka Y, Ohsugi M, Kono N, Ogata F, Yagi N, Ohto
758 U, Kimoto M, Miyake K, et al. Saturated fatty acid and TLR signaling link beta cell
759 dysfunction and islet inflammation. *Cell Metab*. 2012;15:518-33.
760 37. Bergmark BA, Marston NA, Bramson CR, Curto M, Ramos V, Jevne A, Kuder JF,
761 Park JG, Murphy SA, Verma S, et al. Effect of Vupanorsen on Non-High-Density
762 Lipoprotein Cholesterol Levels in Statin-Treated Patients With Elevated Cholesterol:
763 TRANSLATE-TIMI 70. *Circulation*. 2022;145:1377-1386.
764 38. Plump AS, Smith JD, Hayek T, Aalto-Setala K, Walsh A, Verstuyft JG, Rubin EM
765 and Breslow JL. Severe hypercholesterolemia and atherosclerosis in apolipoprotein E-
766 deficient mice created by homologous recombination in ES cells. *Cell*. 1992;71:343-53.
767 39. Ulug P, Powell JT, Martinez MA, Ballard DJ and Filardo G. Surgery for small
768 asymptomatic abdominal aortic aneurysms. *Cochrane Database Syst Rev*.
769 2020;7:CD001835.
770 40. Liu J, Lu H, Howatt DA, Balakrishnan A, Moorleghen JJ, Sorci-Thomas M, Cassis
771 LA and Daugherty A. Associations of ApoAI and ApoB-containing lipoproteins with AngII-
772 induced abdominal aortic aneurysms in mice. *Arterioscler Thromb Vasc Biol*.
773 2015;35:1826-34.
774 41. Ishibashi S, Herz J, Maeda N, Goldstein JL and Brown MS. The two-receptor
775 model of lipoprotein clearance: tests of the hypothesis in "knockout" mice lacking the
776 low density lipoprotein receptor, apolipoprotein E, or both proteins. *Proc Natl Acad Sci U*
777 *S A*. 1994;91:4431-5.
778 42. Ikezoe T, Shoji T, Guo J, Shen F, Lu HS, Daugherty A, Nunokawa M, Kubota H,
779 Miyata M, Xu B, et al. No Effect of Hypercholesterolemia on Elastase-Induced
780 Experimental Abdominal Aortic Aneurysm Progression. *Biomolecules*. 2021;11.
781 43. Yu H, Jiao X, Yang Y, Lv Q, Du Z, Li L, Hu C, Du Y, Zhang J, Li F, et al. ANGPTL8
782 deletion attenuates abdominal aortic aneurysm formation in ApoE-/- mice. *Clin Sci*
783 *(Lond)*. 2023;137:979-993.
784 44. Krishna SM, Seto SW, Moxon JV, Rush C, Walker PJ, Norman PE and Golledge
785 J. Fenofibrate increases high-density lipoprotein and sphingosine 1 phosphate
786 concentrations limiting abdominal aortic aneurysm progression in a mouse model. *Am J*
787 *Pathol*. 2012;181:706-18.

788 45. Golledge J, Cullen B, Rush C, Moran CS, Secomb E, Wood F, Daugherty A,
789 Campbell JH and Norman PE. Peroxisome proliferator-activated receptor ligands
790 reduce aortic dilatation in a mouse model of aortic aneurysm. *Atherosclerosis*.
791 2010;210:51-6.
792 46. Pinchbeck JL, Moxon JV, Rowbotham SE, Bourke M, Lazzaroni S, Morton SK,
793 Matthews EO, Hendy K, Jones RE, Bourke B, et al. Randomized Placebo-Controlled
794 Trial Assessing the Effect of 24-Week Fenofibrate Therapy on Circulating Markers of
795 Abdominal Aortic Aneurysm: Outcomes From the FAME -2 Trial. *J Am Heart Assoc*.
796 2018;7:e009866.
797 47. Hosseini A, Sahranavard T, Reiner Ž, Jamialahmadi T, Dhaheri YA, Eid AH and
798 Sahebkar A. Effect of statins on abdominal aortic aneurysm. *Eur J Pharm Sci*.
799 2022;178:106284.
800 48. Takagi H, Yamamoto H, Iwata K, Goto S and Umemoto T. Effects of statin
801 therapy on abdominal aortic aneurysm growth: a meta-analysis and meta-regression of
802 observational comparative studies. *Eur J Vasc Endovasc Surg*. 2012;44:287-92.
803 49. Salata K, Syed M, Hussain MA, de Mestral C, Greco E, Mamdani M, Tu JV,
804 Forbes TL, Bhatt DL, Verma S, et al. Statins Reduce Abdominal Aortic Aneurysm
805 Growth, Rupture, and Perioperative Mortality: A Systematic Review and Meta-Analysis.
806 *J Am Heart Assoc*. 2018;7:e008657.
807 50. Guo DC, Regalado ES, Gong L, Duan X, Santos-Cortez RL, Arnaud P, Ren Z,
808 Cai B, Hostetler EM, Moran R, et al. LOX Mutations Predispose to Thoracic Aortic
809 Aneurysms and Dissections. *Circ Res*. 2016;118:928-34.
810 51. Kanematsu Y, Kanematsu M, Kurihara C, Tsou TL, Nuki Y, Liang EI, Makino H
811 and Hashimoto T. Pharmacologically induced thoracic and abdominal aortic aneurysms
812 in mice. *Hypertension*. 2010;55:1267-74.
813 52. Yoshimura K, Aoki H, Ikeda Y, Fujii K, Akiyama N, Furutani A, Hoshii Y, Tanaka N,
814 Ricci R, Ishihara T, et al. Regression of abdominal aortic aneurysm by inhibition of c-Jun
815 N-terminal kinase. *Nat Med*. 2005;11:1330-8.
816 53. Hu Y, Fan Y, Zhang C and Wang C. Palmitic acid inhibits vascular smooth muscle
817 cell switch to synthetic phenotype via upregulation of miR-22 expression. *Aging (Albany
818 NY)*. 2022;14:8046-8060.
819 54. Gaudet D, Greber-Platzer S, Reeskamp LF, Iannuzzo G, Rosenson RS, Saheb
820 S, Stefanutti C, Stroes E, Wiegman A, Turner T, et al. Evinacumab in homozygous
821 familial hypercholesterolaemia: long-term safety and efficacy. *Eur Heart J*.
822 2024;45:2422-2434.
823 55. Watts GF, Schwabe C, Scott R, Gladding PA, Sullivan D, Baker J, Clifton P,
824 Hamilton J, Given B, Melquist S, et al. RNA interference targeting ANGPTL3 for
825 triglyceride and cholesterol lowering: phase 1 basket trial cohorts. *Nat Med*.
826 2023;29:2216-2223.

827 56. Gaudet D, Clifton P, Sullivan D, Baker J, Schwabe C, Thackwray S, Scott R,
828 Hamilton J, Given B, Melquist S, et al. RNA Interference Therapy Targeting
829 Apolipoprotein C-III in Hypertriglyceridemia. *NEJM Evid*. 2023;2:EVIDoa2200325.
830 57. Zha Y, Lu Y, Zhang T, Yan K, Zhuang W, Liang J, Cheng Y and Wang Y.
831 CRISPR/Cas9-mediated knockout of APOC3 stabilizes plasma lipids and inhibits
832 atherosclerosis in rabbits. *Lipids Health Dis*. 2021;20:180.
833 58. Zuo Y, Zhang C, Zhou Y, Li H, Xiao W, Herzog RW, Xu J, Zhang J, Chen YE and
834 Han R. Liver-specific in vivo base editing of Angptl3 via AAV delivery efficiently lowers
835 blood lipid levels in mice. *Cell Biosci*. 2023;13:109.
836 59. Baass A, Paquette M, Bernard S and Hegele RA. Familial chylomicronemia
837 syndrome: an under-recognized cause of severe hypertriglyceridaemia. *J Intern Med*.
838 2020;287:340-348.
839 60. Miller M, Stone NJ, Ballantyne C, Bittner V, Criqui MH, Ginsberg HN, Goldberg
840 AC, Howard WJ, Jacobson MS, Kris-Etherton PM, et al. Triglycerides and
841 cardiovascular disease: a scientific statement from the American Heart Association.
842 *Circulation*. 2011;123:2292-333.

843

Figures

Fig. 1: Mendelian Randomization identifies circulating proteins and metabolites causally related to AAA risk.

A, Outline of the analyses performed. Two-sample Mendelian Randomization (MR) analyses were applied to determine the causal effects of circulating proteins, and nuclear magnetic resonance (NMR) measured circulating metabolites on the risk of abdominal aortic aneurysm (AAA) using multiple data sources. **B**, Forest plot displaying the causal effects of 41 proteins identified through MR-Wald ratio analysis after Bonferroni correction. **C**, Classifications of NMR metabolites and the relative lipid compositions of the 14 lipoprotein subclasses (left). All 14 lipoprotein subclass particles are illustrated using the same size scale, with diameters based on mean values from 5,651 participants in the Northern Finland Birth Cohort 1966 (NFBC66). Note that the size of the LDL and HDL particles in the figure is multiplied by 1.5 and 2.0, respectively. The right side features a circular histplot of the MR results for 141 metabolites. Each bar's height represents the absolute effect size, while the color indicates the direction and P-value as determined by the MR inverse-variance weighted (IVW) method.

Fig. 2: Impaired LPL activity accelerates AAA development and aortic rupture.

A, Design of the AAA study in *Lpl*-deficient mice. Inducible global *Lpl*-deficient mice were generated by crossing *Lpl* floxed ($Lpl^{f/f}$) mice with β-actin driven tamoxifen-inducible MerCreMer transgenic mice. Low cholesterol, Western diet feeding was initiated 2 weeks after the start of tamoxifen treatment. **B**, Aortic rupture incidence curve during 4 weeks of AngII infusion. **C**, Aortic aneurysm incidence in $Lpl^{f/f}$ (n=11) and i$Lpl^{-/-}$ (n=10) mice. **D**, Design of the AAA study in *Apoa5*-deficient mice. Mice were fed a standard rodent laboratory diet. After 4-week of AngII infusion, aortas from surviving mice were harvested. **E**, Representative aorta of male WT (n = 14) and *Apoa5*-deficient (n = 15) mice after 4 weeks of AngII infusion. Plasma samples were collected on day 28 and subjected individually to analytical chemistry to measure triglycerides (TG) and total cholesterol (TC). **F-J**, The TG (**F**), TC (**G**), maximal aortic diameter (**H**), AAA incidence (**I**), and systolic blood pressure (**J**) in male mice. **K-O**, TG (**K**), TC (**L**), maximal aortic diameter (**M**), AAA incidence (**N**), and systolic blood pressure (**O**) in female WT (n = 10) and *Apoa5*-deficient (n = 8) mice in AngII-induced AAA study. Data are presented as circles and Mean ± SEM (**F-H**, **J -M**, **O**). Statistical analyses were conducted as follows: Chi-Squared test for **C**, **I**, **N**; Mann-Whitney U test for **F**, **M**; Student's t-test for **G**, **H**, **K**, **L**; Kruskal-Wallis test followed by Dunn's post hoc analysis for **J**; One-way ANOVA followed by Sidak post hoc analysis for **O**. SBP, systolic blood pressure.

880 **Fig. 3: Dramatically increased TG concentrations accelerate AAA development**
881 **and dissection in h*APOC3* Tg mice.**

882 **A**, Design of the AAA study in human *APOC3* transgenic (h*APOC3* Tg) mice. Twelve- to
883 16-week-old h*APOC3* Tg mice (n of male = 15; n of female = 24) or WT littermates (n of
884 male = 17, n of female =21) were infused with AngII (1,000 ng/kg/min) for 4 weeks to
885 induce AAA. Systolic blood pressures were measured before and after AngII infusion.
886 The mice were fed a standard rodent laboratory diet. After 4 weeks, aortas from
887 surviving mice were harvested. Plasma samples were collected on day 28 and
888 subjected individually to analytical chemistry. **B**-**D**, plasma triglycerides (TG) (**B**), total
889 cholesterol (TC) (**C**), and non-esterified fatty acids (**D**) in male mice. Representative
890 aortas of male WT and h*APOC3* Tg mice after 4 weeks of AngII infusion (**E**). Maximal
891 aortic diameter (**F**), AAA incidence (**G**), dissection rate (**H**), and systolic blood pressure
892 (**I**) in male mice. **J**-**Q**, The TG (**J**), TC (**K**), non-esterified fatty acids (**L**), maximal aortic
893 diameter (**M**), AAA incidence (**N**), and dissection rate (**O**) in female WT and h*APOC3* Tg
894 mice after 4 weeks of AngII infusion. Data are presented as circles and Mean ± SEM (**B-**
895 **D**, **F**, **I-M**). Statistical analyses were conducted as follows: Mann-Whitney U test for **B**,
896 **D**, **F**, **J**, **K**; Student's t-test for **C**, **L**, **M**; Chi-Squared test for **G**, **H**, **N**, **O**; One-way
897 ANOVA followed by Sidak post hoc analysis for **I**. Scale bars: 1 mm in **E**. SBP, systolic
898 blood pressure; NEFA, non-esterified fatty acids.

899

900 **Fig. 4: Palmitic acid inhibits LOX maturation in HASMCs and aortas.**

901 **A,** Two-sample mendelian randomization to detect the causal effects of TG on
902 circulating total fatty acid, palmitic acid (PA, 16:0), stearic acid (18:0), palmitoleic acid
903 (16:1n-7), and oleic acid (18:1n-9) levels. **B**, Untargeted metabolomics was applied to
904 measure the ethyl palmitate levels in plasma from 14-18-week-old male h*APOC3* Tg
905 (heterozygous) mice and littermate controls. **C-G**, Human aortic smooth muscle cells
906 (HASMCs) were starved in OptiMEM-reduced serum medium for 24 hours, followed by
907 incubation with palmitic acid (250 μM; PA) or vehicle (BSA) for another 24 hours. Total
908 RNA was extracted for RNA sequencing or qRT-PCR. **C,** Reactome pathway enrichment
909 analysis of down-regulated genes in the PA group. **D**, Top 5 downregulated Reactome
910 pathways identified from Gene Set Enrichment Analysis (GSEA). **E**, Heatmap of gene
911 expression levels involved in elastic fiber formation and maturation. qRT-PCR analysis
912 of *LOX* (**F**) and *BMP1* (**G**) (data from 4 independent experiments). **H**, Correlation
913 between liver *APOC3* expression level and aortic *BMP1* expression level among 131
914 donors in the GTEx project. **I-J**, HASMCs were starved in OptiMEM for 24 hours, then
915 incubated with PA (250 μM) or vehicle along with TGF-β (10 ng/ml) or vehicle for
916 another 24 hours; Or, HASMCs were transfected with adenovirus GFP or LOX (30 MOI)

917 for 6 hours in a growth medium, then starved in OptiMEM for another 24 hours. Cells
918 were incubated with PA (250 μM) or vehicle for an additional 24 hours. Conditioned
919 medium was collected for Western blot analysis. Cell total DNA was used for
920 normalization. **I**, Representative Western blot image of mature LOX in conditioned
921 medium. **J**, Quantification analysis of mature LOX protein abundance. **K-L,** HASMC
922 were transfected with siBMP1 at 1 nM or siCtr with RNAimax for 6 hours in OptiMEM-
923 reduced serum medium, then transfected with adenovirus GFP or LOX (30 MOI) for
924 another 23 hours in OptiMEM-reduced serum medium. The condition mediumed was
925 used for Western blot analysis and whole cells were used for RNA extraction or DNA
926 extraction. **K**, qRT-PCR analysis of *BMP1*. **L**, Representative LOX expression in
927 conditioned medium (upper) and quantification analysis (bottom). **M**, Eight-week-old
928 male C57BL/6J mice were given saline, vehicle, or ethyl palmitate (600 mg/kg) for 5
929 consecutive days via intraperitoneal injection. On day 6, mice were euthanized,
930 suprarenal abdominal aortas were isolated, and total protein was extracted and
931 analyzed by Western blot to detect LOX abundance in suprarenal abdominal aortas,
932 with corresponding quantifications for mature LOX (n = 5/group). **N**, Twelve- to 16-week-
933 old h*APOC3* Tg mice and littermate control mice were infused with saline or AngII
934 (1,000 ng/kg/min) for 7 days. On day 8, mice were euthanized, suprarenal abdominal
935 aortas were isolated, and total protein was extracted and analyzed by Western blot to
936 detect LOX expression in suprarenal abdominal aortas, with corresponding
937 quantifications for mature LOX (n = 3 or 4/genotyping/treatment). Data are presented as
938 dots and Mean ± SEM (**B**, **F-G**, **J-N**). Statistical analyses were conducted as follows:
939 One-way ANOVA followed by Sidak post hoc analysis for **K, M, N**. Student's t-test for **B,**
940 **F**, **G**; Mann-Whitney U test followed by Bonferroni correction for **J, L.**

941

942 **Fig. 5: LOX Overexpression Inhibits AAA formation and dissection in *hAPOC3* Tg**
943 **Mice**

944 **A**, Design of the LOX overexpression (OE) study in human *APOC3* Tg mice. Twelve- to
945 16-week-old male h*APOC3* Tg mice and their littermates WT controls were transfected
946 with $9x10^8$ pfu adnovirus GFP or LOX to the suprarenal abdominal aorta then infused
947 with AngII (1,000 ng/kg/min) for 18 days to induce AAA. **B**, Representative aortic trees
948 from the 4 groups. **E-F**, Quantifications of AAA incidence (**E**), dissection rate (**F**), and
949 maximal aorta diameter (**G**) among the 4 groups. Systolic blood pressure (**H**), body
950 weight (**I**), plasma triglycerides (TG) (**J**), total cholesterol (**K**), and non-esterified fatty
951 acids (**L**). **M**, Representative Masson's trichrome, Verhoeff-Van Gieson (VVG), and H&E
952 staining of suprarenal abdominal aorta sections. Data are presented as dots and Mean
953 ± SEM (**E-J**). Statistical analyses were conducted as follows: Chi-Squared test for **C, D**;

954 One-way ANOVA followed by Sidak post hoc analysis for **E-G, I-J;** Kruskal-Wallis test
955 followed by Dunn's post hoc analysis for **H**. Scale bars: 1 mm in **B**, 100 μm in **K**.

956

957 **Fig. 6: Administration of *Angptl3* ASO prevents AAA formation in h*APOC3* Tg**
958 **mice.**

959 **A**, Design of the *Angptl3* ASO study in human *APOC3* Tg mice. Twelve- to 16-week-old
960 male h*APOC3* Tg mice were given one injection of *Angptl3* ASO (10 mg/kg) or
961 scrambled ASO by subcutaneous administration. After 3 days, mice were infused with
962 AngII (1,000 ng/kg/min) for 25 days. Three more injections (3 mg/kg) were conducted
963 on days 7, 14, and 21. A wild-type group was included, receiving injections of scramble
964 ASO. At the end of the study, aortas, livers, and plasma were harvested. **B**, Relative
965 abundance of *Angptl3* mRNA in livers of the three groups. **C-D**, Plasma ANGPTL3
966 protein concentrations (**C**) and non-esterified fatty acids (**D**) at the endpoint. **E** to **F**,
967 Plasma triglycerides (TG) (**E**) and total cholesterol (TC) (**F**) concentrations on days 0, 3,
968 and 28. **G**, Representative aortic trees from the 3 groups. **H**, Representative H&E
969 staining (left) and Verhoeff-Van Gieson (VVG) staining (right) of suprarenal abdominal
970 aorta sections. **I-L**, Quantifications of AAA incidence (**I**), maximal aorta diameter (**J**),
971 elastic fiber degradation score (**K**), and dissection rate (**L**) among the 3 groups. **M**,
972 Relative abundance of *Apoc3* in the liver. **N**, Plasma mouse-specific APOC3
973 concentrations were measured by ELISA at the endpoint. **O**, Relative liver abundance of
974 human *APOC3*. **P**, Plasma human APOC3 concentrations were determined by ELISA at
975 the endpoint. **Q**, Body weight comparisons among the 3 groups before and at the end of
976 the study. **R**, Systolic blood pressure comparisons among the 3 groups before and at
977 the end of the study. Data are presented as circles/dots and Mean ± SEM or Mean only.
978 Statistical analyses were conducted as follows: One-way ANOVA followed by Sidak post
979 hoc analysis for **B**, **C**, **D**, **E,** day 3 of **F, M, N, R**; Kruskal-Wallis test followed by Dunn's
980 post hoc analysis for day 0 and 28 of **F, J**, **K**, **O**, **P, Q**; Chi-Squared test for **I**, **L**. Scale
981 bars: 1 mm in **G**, 100 μm in **H**. SBP, systolic blood pressure; NEFA, non-esterified fatty
982 acids; #, $P < 0.005$ of the comparison of Ctr and WT group. *, $P < 0.005$ of the
983 comparison of Ctr and ASO group.

984

985 **Fig. 7: Administration of *Angptl3* ASO prevents AAA formation in *Apoe*-deficient**
986 **mice.**

987 **A**, Design of the *Angptl3* ASO study in male *Apoe*-deficient mice. Ten-week-old male
988 *Apoe*-deficient mice were given a subcutaneous injection of *Angptl3* ASO (10 mg/kg; n =
989 13) or scrambled ASO (n = 12). After 3 days, mice were infused with AngII (1,000

990 ng/kg/min) for 25 days. Three more injections were administered on days 7, 14, and 21.
991 At the end of the study, aortas, livers, and plasma were harvested. **B**, Relative
992 abundance of *Angptl3* mRNA in the liver. **C-D**, Plasma ANGPTL3 protein concentrations
993 (**C**), and non-esterified fatty acids (**D**) at the endpoint. **E,** Plasma triglycerides (TG)
994 levels on days 0, 3, and 28. **F**, Plasma total cholesterol (TC) concentrations on days 3
995 and 28. **G**, Systolic blood pressure before and after AngII infusion. **H**, Body weight
996 changes. TG (**I**) and cholesterol (**J**) concentrations of size exclusion chromatography
997 fractionated plasma from animals (n = 4 in the control group, n = 4 in the *Angptl3* ASO
998 group) determined by enzymatic assays. Fractions 8 to 11 contained VLDL, fractions 12
999 to 17 contained IDL and LDL, and fractions 22 to 25 contained HDL. **K**, Representative
1000 aortic images from the 2 groups. **N-O**, Quantification of AAA incidence (**N**) and maximal
1001 aortic diameter (**O**). **P**, Relative liver mRNA abundance of genes related to VLDL
1002 production (*Apob, Mttp, Srebp1c, Scd, Fasn*), TG lipolysis (*Apoc2, Apoc3, Apoa5, Lpl*),
1003 and TC regulation (*Pcsk9, Ldlr, Lrp1*). Data are presented as circles/dots and/or Mean ±
1004 SEM. Statistical analyses were conducted as follows: Student's t-test for **B**, **C**, day 0
1005 and 28 of **E**, day 28 of **F**; Mann-Whitney U test for **D**, day 3 of **E** and **F**, **O**; One-way
1006 ANOVA followed by Sidak post hoc analysis for **G**; Chi-Squared test for **N;** Student's t-
1007 test or Mann-Whitney U test for **P**. Scale bars: 1 mm in **K**. SBP, systolic blood pressure;
1008 NEFA, non-esterified fatty acids.

Figure 1

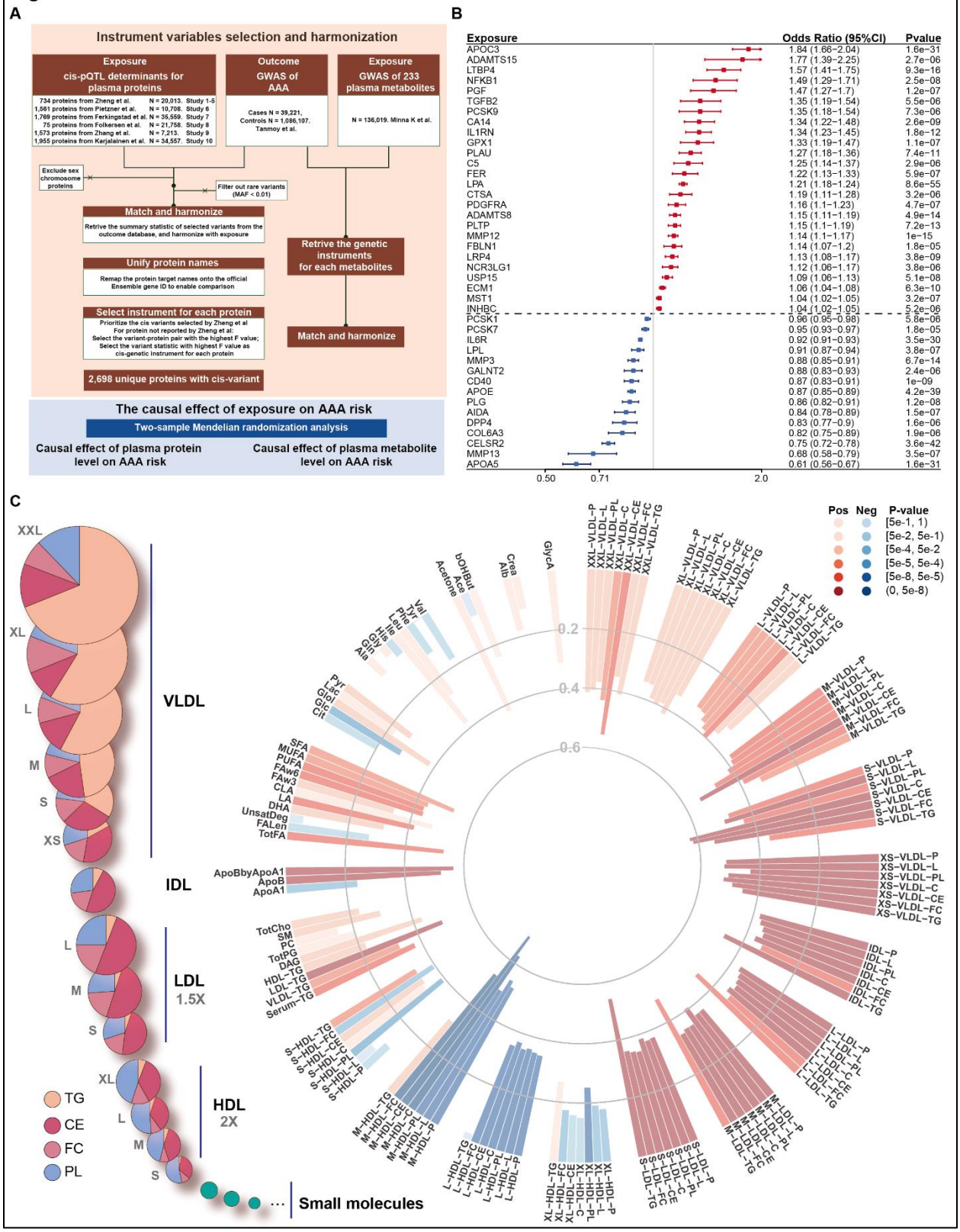
A
Instrument variables selection and harmonization
Exposure
cis-pQTL determinants for plasma proteins
734 proteins from Zheng et al. N = 20,013. Study 1-5
1,561 proteins from Pietzner et al. N = 10,708. Study 6
1,769 proteins from Ferkingstad et al. N = 35,559. Study 7
75 proteins from Folkersen et al. N = 21,758. Study 8
1,573 proteins from Zhang et al. N = 7,213. Study 9
1,955 proteins from Karjalainen et al. N = 34,557. Study 10
Outcome
GWAS of AAA
Cases N = 39,221, Controls N = 1,086,107. Tanmoy et al.
Exposure
GWAS of 233 plasma metabolites
N = 136,019. Minna K et al.
Exclude sex chromosome proteins
Filter out rare variants (MAF < 0.01)
Match and harmonize
Retrive the summary statistic of selected variants from the outcome database, and harmonize with exposure
Unify protein names
Remap the protein target names onto the official Ensemble gene ID to enable comparison
Select instrument for each protein
Prioritize the cis variants selected by Zheng et al
For protein not reported by Zheng et al:
Select the variant-protein pair with the highest F value;
Select the variant statistic with highest F value as cis-genetic instrument for each protein
2,698 unique proteins with cis-variant
Retrive the genetic instruments for each metabolites
Match and harmonize
The causal effect of exposure on AAA risk
Two-sample Mendelian randomization analysis
Causal effect of plasma protein level on AAA risk
Causal effect of plasma metabolite level on AAA risk
B
Exposure
Odds Ratio (95%CI)
Pvalue
APOC3 1.84 (1.66−2.04) 1.6e−31
ADAMTS15 1.77 (1.39−2.25) 2.7e−06
LTBP4 1.57 (1.41−1.75) 9.3e−16
NFKB1 1.49 (1.29−1.71) 2.5e−08
PGF 1.47 (1.27−1.7) 1.2e−07
TGFB2 1.35 (1.19−1.54) 5.5e−06
PCSK9 1.35 (1.18−1.54) 7.3e−06
CA14 1.34 (1.22−1.48) 2.6e−09
IL1RN 1.34 (1.23−1.45) 1.8e−12
GPX1 1.33 (1.19−1.47) 1.1e−07
PLAU 1.27 (1.18−1.36) 7.4e−11
C5 1.25 (1.14−1.37) 2.9e−06
FER 1.22 (1.13−1.33) 5.9e−07
LPA 1.21 (1.18−1.24) 8.6e−55
CTSA 1.19 (1.11−1.28) 3.2e−06
PDGFRA 1.16 (1.1−1.23) 4.7e−07
ADAMTS8 1.15 (1.11−1.19) 4.9e−14
PLTP 1.15 (1.1−1.19) 7.2e−13
MMP12 1.14 (1.1−1.17) 1e−15
FBLN1 1.14 (1.07−1.2) 1.8e−05
LRP4 1.13 (1.08−1.17) 3.8e−09
NCR3LG1 1.12 (1.06−1.17) 3.8e−06
USP15 1.09 (1.06−1.13) 5.1e−08
ECM1 1.06 (1.04−1.08) 6.3e−10
MST1 1.04 (1.02−1.05) 3.2e−07
INHBC 1.04 (1.02−1.05) 5.2e−06
PCSK1 0.96 (0.95−0.98) 5.8e−06
PCSK7 0.95 (0.93−0.97) 1.8e−05
IL6R 0.92 (0.91−0.93) 3.5e−30
LPL 0.91 (0.87−0.94) 3.8e−07
MMP3 0.88 (0.85−0.91) 6.7e−14
GALNT2 0.88 (0.83−0.93) 2.4e−06
CD40 0.87 (0.83−0.91) 1e−09
APOE 0.87 (0.85−0.89) 4.2e−39
PLG 0.86 (0.82−0.91) 1.2e−08
AIDA 0.84 (0.78−0.89) 1.5e−07
DPP4 0.83 (0.77−0.9) 1.6e−06
COL6A3 0.82 (0.75−0.89) 1.9e−06
CELSR2 0.75 (0.72−0.78) 3.6e−42
MMP13 0.68 (0.58−0.79) 3.5e−07
APOA5 0.61 (0.56−0.67) 1.6e−31
0.50
0.71
2.0
C
Pos Neg P-value
[5e-1, 1)
[5e-2, 5e-1)
[5e-4, 5e-2
[5e-5, 5e-4)
[5e-8, 5e-5)
(0, 5e-8)
XXL
XL
L
M
S
XS
VLDL
IDL
LDL
1.5X
HDL
2X
Small molecules
TG
CE
FC
PL
0.2
0.4
0.6
GlycA
Crea
Alb
bOHBut
Ace
Acetone
Val
Tyr
Phe
Leu
Ile
His
Gln
Ala
Alb
Pyr
Lac
Fol
Gly
Cit
SFA
MUFA
PUFA
FAw6
FAw3
CLA
LA
DHA
UnsatDeg
FALen
TotFA
ApoBbyApoA1
ApoB
ApoA1
TotCho
SM
PC
TotPG
DAG
HDL-TG
LDL-TG
VLDL-TG
Serum-TG
XXL-VLDL-P
XXL-VLDL-L
XXL-VLDL-PL
XXL-VLDL-C
XXL-VLDL-CE
XXL-VLDL-FC
XXL-VLDL-TG
XL-VLDL-P
XL-VLDL-L
XL-VLDL-PL
XL-VLDL-C
XL-VLDL-CE
XL-VLDL-FC
XL-VLDL-TG
L-VLDL-P
L-VLDL-L
L-VLDL-PL
L-VLDL-C
L-VLDL-CE
L-VLDL-FC
L-VLDL-TG
M-VLDL-P
M-VLDL-L
M-VLDL-PL
M-VLDL-C
M-VLDL-CE
M-VLDL-FC
M-VLDL-TG
S-VLDL-P
S-VLDL-L
S-VLDL-PL
S-VLDL-C
S-VLDL-CE
S-VLDL-FC
S-VLDL-TG
XS-VLDL-P
XS-VLDL-L
XS-VLDL-PL
XS-VLDL-C
XS-VLDL-CE
XS-VLDL-FC
XS-VLDL-TG
IDL-P
IDL-L
IDL-PL
IDL-C
IDL-CE
IDL-FC
IDL-TG
L-LDL-P
L-LDL-L
L-LDL-PL
L-LDL-C
L-LDL-CE
L-LDL-FC
L-LDL-TG
M-LDL-P
M-LDL-L
M-LDL-PL
M-LDL-C
M-LDL-CE
M-LDL-FC
M-LDL-TG
S-LDL-P
S-LDL-L
S-LDL-PL
S-LDL-C
S-LDL-CE
S-LDL-FC
S-LDL-TG
XL-HDL-P
XL-HDL-L
XL-HDL-PL
XL-HDL-C
XL-HDL-CE
XL-HDL-FC
XL-HDL-TG
L-HDL-P
L-HDL-L
L-HDL-PL
L-HDL-C
L-HDL-CE
L-HDL-FC
L-HDL-TG
M-HDL-P
M-HDL-L
M-HDL-PL
M-HDL-C
M-HDL-CE
M-HDL-FC
M-HDL-TG
S-HDL-P
S-HDL-L
S-HDL-PL
S-HDL-C
S-HDL-CE
S-HDL-FC
S-HDL-TG

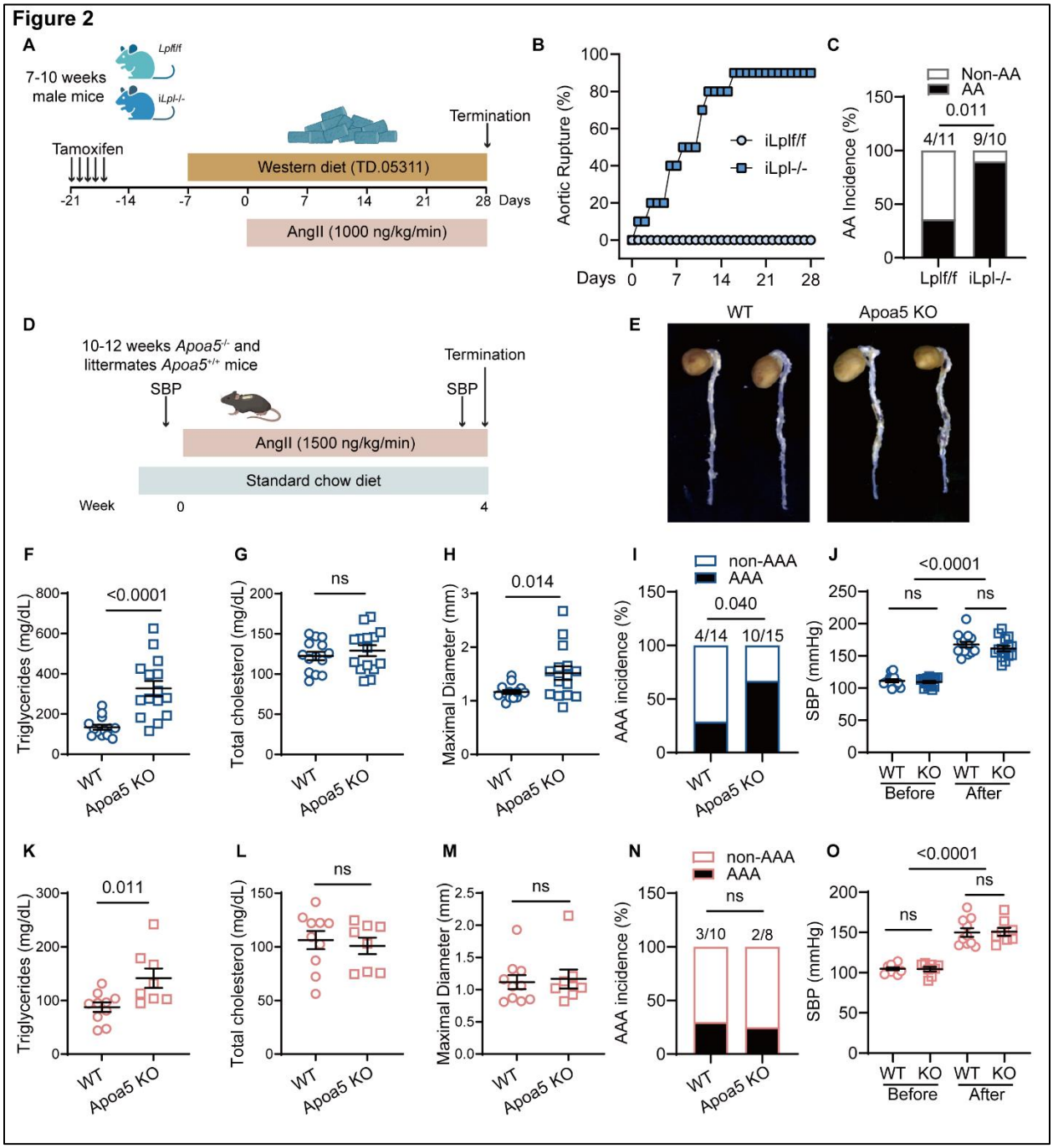
Figure 2
A
7-10 weeks male mice
Lpl f/f
iLpl-/-
Tamoxifen
Western diet (TD.05311)
Termination
-21 -14 -7 0 7 14 21 28 Days
AngII (1000 ng/kg/min)
B
Aortic Rupture (%)
iLplf/f
iLpl-/-
Days 0 7 14 21 28
C
Non-AA
AA
0.011
4/11 9/10
AA Incidence (%)
Lplf/f iLpl-/-
D
10-12 weeks Apoa5-/- and littermates Apoa5+/+ mice
SBP
Termination
SBP
AngII (1500 ng/kg/min)
Standard chow diet
Week 0 4
E
WT
Apoa5 KO
F
<0.0001
Triglycerides (mg/dL)
WT Apoa5 KO
G
ns
Total cholesterol (mg/dL)
WT Apoa5 KO
H
0.014
Maximal Diameter (mm)
WT Apoa5 KO
I
non-AAA
AAA
0.040
4/14 10/15
AAA incidence (%)
WT Apoa5 KO
J
<0.0001
ns ns
SBP (mmHg)
WT KO WT KO
Before After
K
0.011
Triglycerides (mg/dL)
WT Apoa5 KO
L
ns
Total cholesterol (mg/dL)
WT Apoa5 KO
M
ns
Maximal Diameter (mm)
WT Apoa5 KO
N
non-AAA
AAA
ns
3/10 2/8
AAA incidence (%)
WT Apoa5 KO
O
<0.0001
ns ns
SBP (mmHg)
WT KO WT KO
Before After

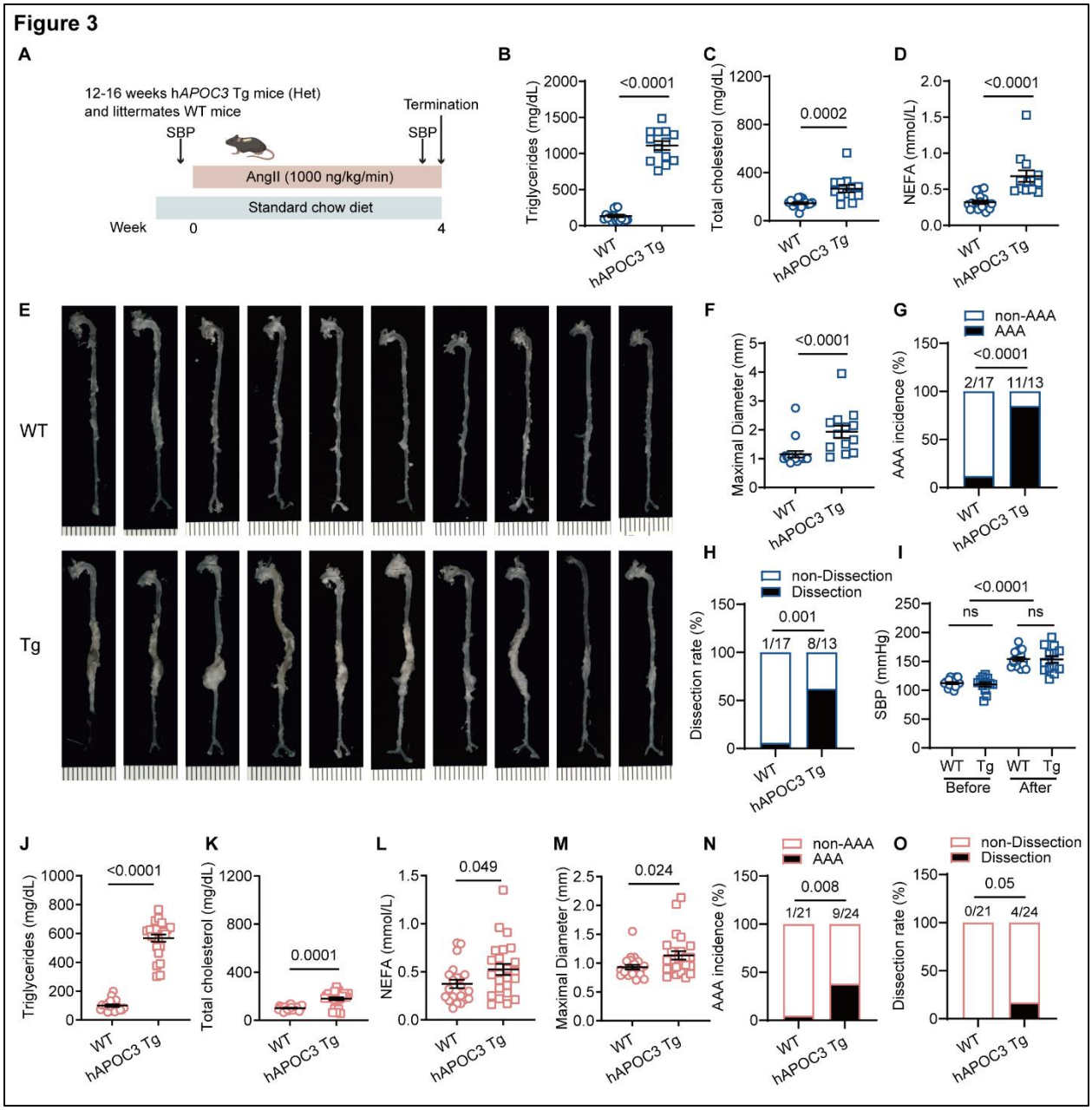
Figure 3
A
12-16 weeks hAPOC3 Tg mice (Het)
and littermates WT mice
SBP
Termination
SBP
AngII (1000 ng/kg/min)
Standard chow diet
Week
0
4
B
Triglycerides (mg/dL)
<0.0001
WT
hAPOC3 Tg
C
Total cholesterol (mg/dL)
0.0002
D
NEFA (mmol/L)
<0.0001
E
WT
Tg
F
Maximal Diameter (mm)
<0.0001
G
non-AAA
AAA
AAA incidence (%)
<0.0001
2/17
11/13
H
non-Dissection
Dissection
Dissection rate (%)
0.001
1/17
8/13
I
SBP (mmHg)
<0.0001
ns
ns
WT
Tg
Before
After
J
Triglycerides (mg/dL)
<0.0001
K
Total cholesterol (mg/dL)
0.0001
L
NEFA (mmol/L)
0.049
M
Maximal Diameter (mm)
0.024
N
non-AAA
AAA
AAA incidence (%)
0.008
1/21
9/24
O
non-Dissection
Dissection
Dissection rate (%)
0.05
0/21
4/24

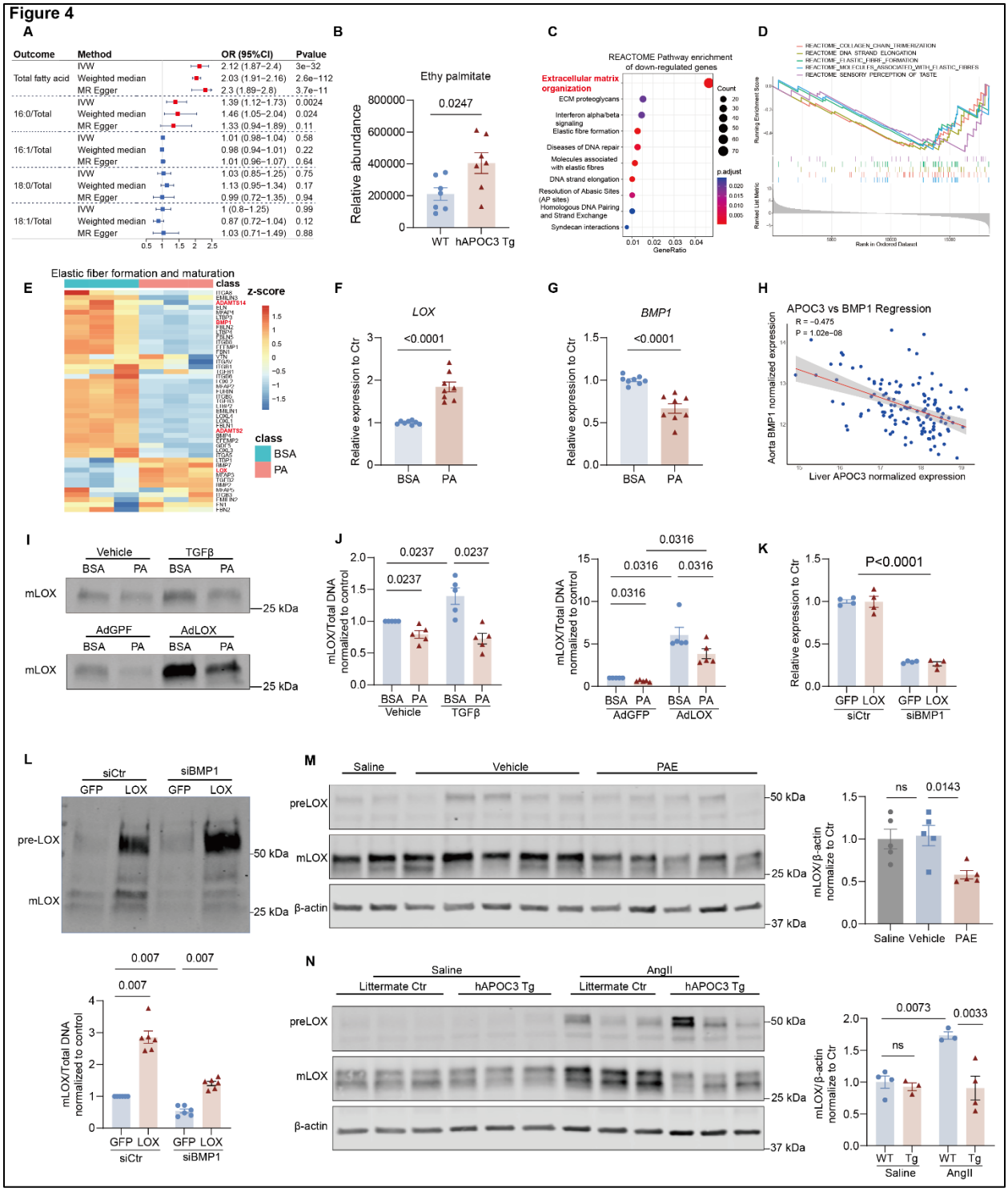
Figure 4
A
Outcome
Method
OR (95%CI)
Pvalue
Total fatty acid
IVW
2.12 (1.87–2.4)
3e−32
Weighted median
2.03 (1.91–2.16)
2.6e−112
MR Egger
2.3 (1.89–2.8)
3.7e−11
16:0/Total
IVW
1.39 (1.12–1.73)
0.0024
Weighted median
1.46 (1.05–2.04)
0.024
MR Egger
1.33 (0.94–1.89)
0.11
16:1/Total
IVW
1.01 (0.98–1.04)
0.58
Weighted median
0.98 (0.94–1.01)
0.22
MR Egger
1.01 (0.96–1.07)
0.64
18:0/Total
IVW
1.03 (0.85–1.25)
0.75
Weighted median
1.13 (0.95–1.34)
0.17
MR Egger
0.99 (0.72–1.35)
0.94
18:1/Total
IVW
1 (0.8–1.25)
0.99
Weighted median
0.87 (0.72–1.04)
0.12
MR Egger
1.03 (0.71–1.49)
0.88
B
Ethy palmitate
0.0247
Relative abundance
WT
hAPOC3 Tg
C
REACTOME Pathway enrichment of down-regulated genes
Extracellular matrix organization
ECM proteoglycans
Interferon alpha/beta signaling
Elastic fibre formation
Diseases of DNA repair
Molecules associated with elastic fibres
DNA strand elongation
Resolution of Abasic Sites (AP sites)
Homologous DNA Pairing and Strand Exchange
Syndecan interactions
Count
p.adjust
GeneRatio
D
REACTOME_COLLAGEN_CHAIN_TRIMERIZATION
REACTOME_DNA_STRAND_ELONGATION
REACTOME_ELASTIC_FIBRE_FORMATION
REACTOME_MOLECULES_ASSOCIATED_WITH_ELASTIC_FIBRES
REACTOME_SENSORY_PERCEPTION_OF_TASTE
Running Enrichment Score
Ranked List Metric
Rank in Ordered Dataset
E
Elastic fiber formation and maturation
class
z-score
BSA
PA
F
LOX
<0.0001
Relative expression to Ctr
BSA
PA
G
BMP1
<0.0001
Relative expression to Ctr
BSA
PA
H
APOC3 vs BMP1 Regression
R = −0.475
P = 1.02e−08
Aorta BMP1 normalized expression
Liver APOC3 normalized expression
I
Vehicle
TGFβ
BSA
PA
mLOX
25 kDa
AdGPF
AdLOX
J
0.0237
0.0237
0.0237
mLOX/Total DNA normalized to control
Vehicle
TGFβ
0.0316
0.0316
0.0316
0.0316
AdGPF
AdLOX
K
P<0.0001
Relative expression to Ctr
GFP
LOX
siCtr
siBMP1
L
siCtr
siBMP1
GFP
LOX
pre-LOX
mLOX
50 kDa
25 kDa
0.007
0.007
0.007
mLOX/Total DNA normalized to control
M
Saline
Vehicle
PAE
preLOX
mLOX
β-actin
50 kDa
25 kDa
37 kDa
ns
0.0143
mLOX/β-actin normalize to Ctr
N
Saline
AngII
Littermate Ctr
hAPOC3 Tg
0.0073
0.0033
ns
WT
Tg

Figure 5

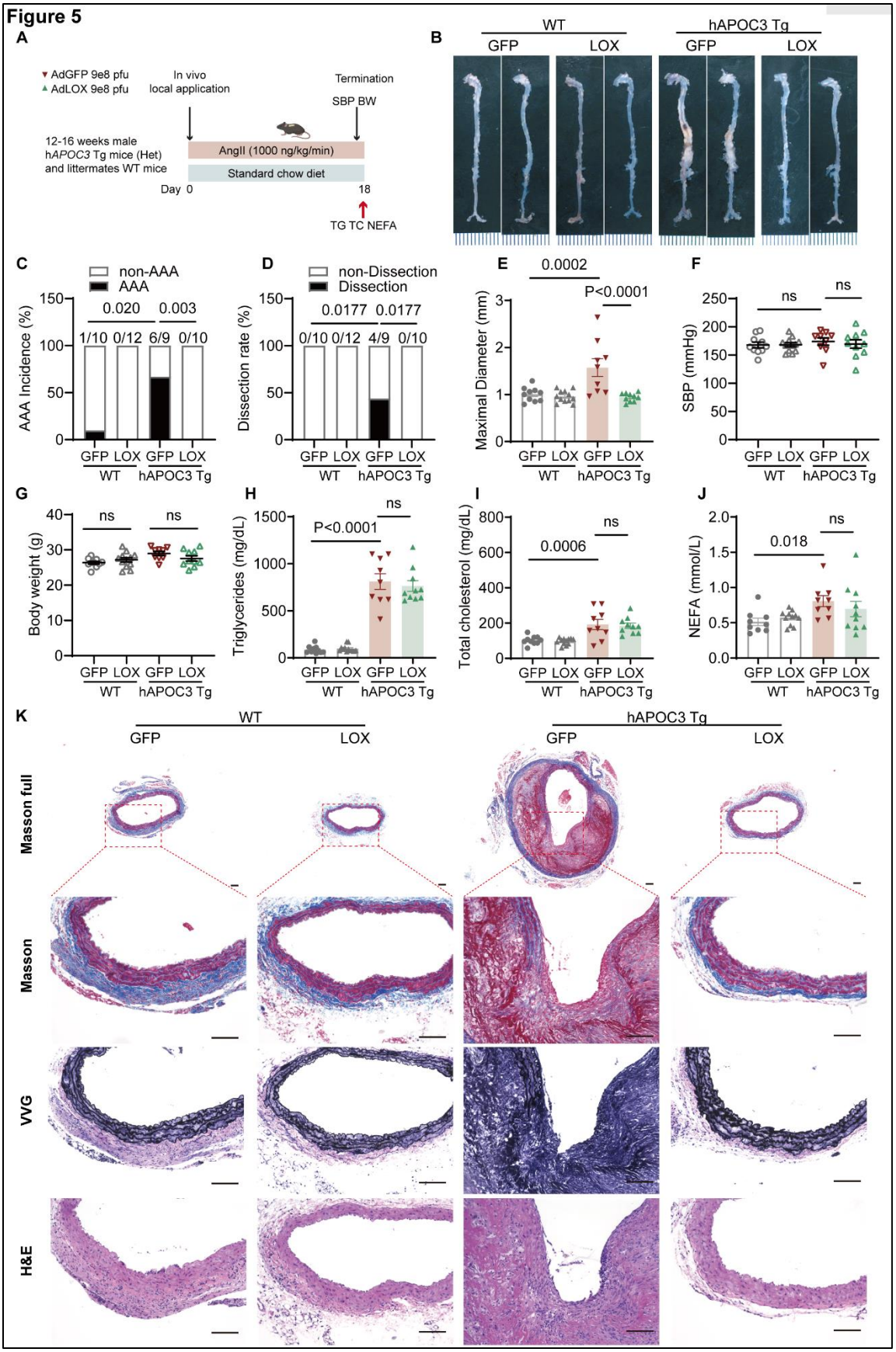
A
AdGFP 9e8 pfu
AdLOX 9e8 pfu
In vivo
local application
Termination
SBP BW
12-16 weeks male
hAPOC3 Tg mice (Het)
and littermates WT mice
AngII (1000 ng/kg/min)
Standard chow diet
Day 0
18
TG TC NEFA
B
WT
hAPOC3 Tg
GFP
LOX
C
non-AAA
AAA
AAA Incidence (%)
0.020
0.003
1/10 0/12 6/9 0/10
D
non-Dissection
Dissection
Dissection rate (%)
0.0177 0.0177
0/10 0/12 4/9 0/10
E
Maximal Diameter (mm)
0.0002
P<0.0001
F
SBP (mmHg)
ns
ns
G
Body weight (g)
ns
ns
H
Triglycerides (mg/dL)
P<0.0001
ns
I
Total cholesterol (mg/dL)
0.0006
ns
J
NEFA (mmol/L)
0.018
ns
GFP LOX GFP LOX
WT hAPOC3 Tg
K
Masson full
Masson
VVG
H&E

Figure 6

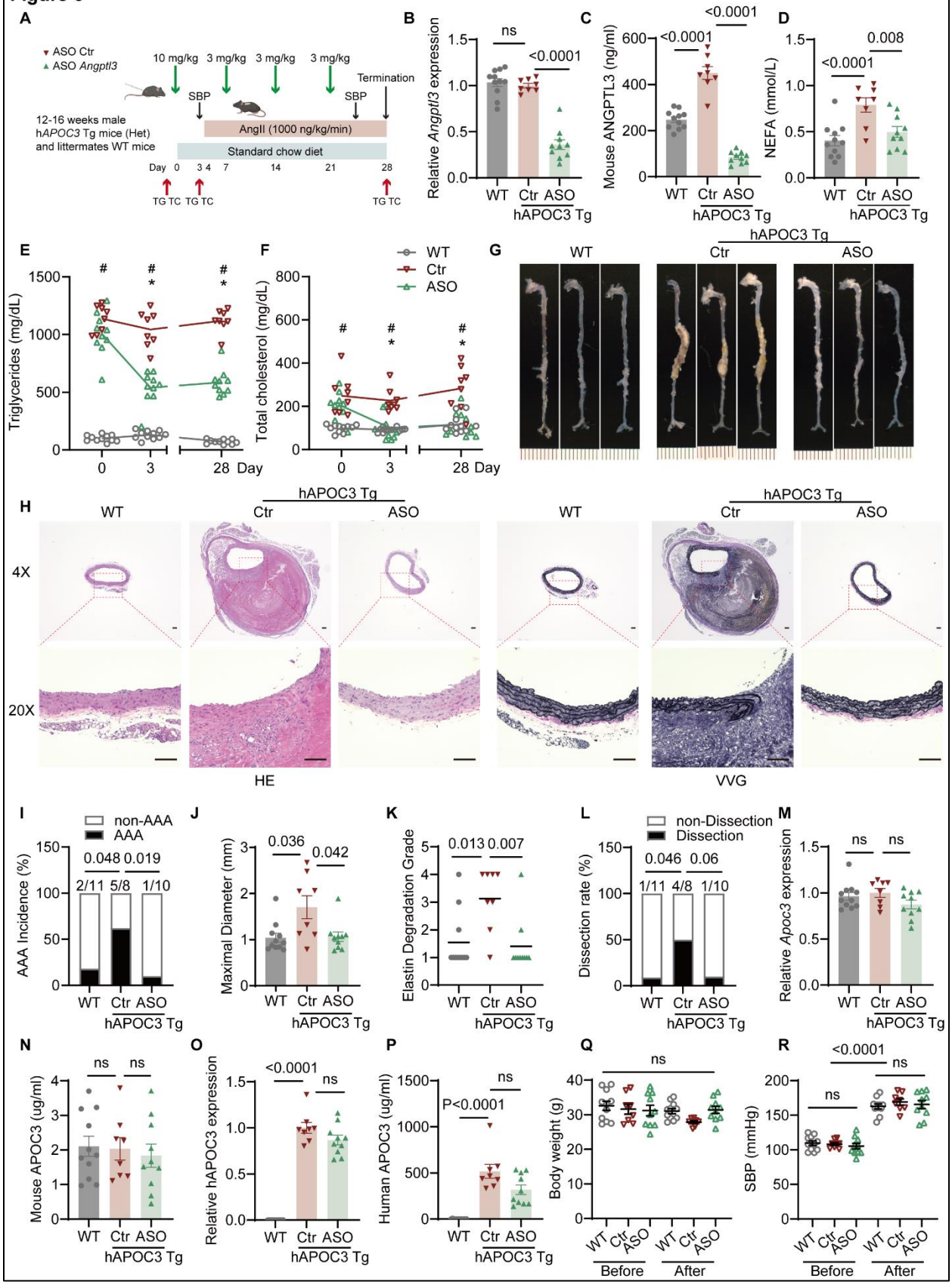
A
ASO Ctr
ASO Angptl3
10 mg/kg
3 mg/kg
3 mg/kg
3 mg/kg
SBP
SBP
Termination
12-16 weeks male
hAPOC3 Tg mice (Het)
and littermates WT mice
AngII (1000 ng/kg/min)
Standard chow diet
Day 0 3 4 7 14 21 28
TG TC TG TC
TG TC
B
Relative Angptl3 expression
ns
<0.0001
C
Mouse ANGPTL3 (ng/ml)
<0.0001
<0.0001
D
NEFA (mmol/L)
<0.0001
0.008
WT Ctr ASO
hAPOC3 Tg
E
Triglycerides (mg/dL)
Day
F
Total cholesterol (mg/dL)
WT
Ctr
ASO
G
H
4X
20X
HE
VVG
I
non-AAA
AAA
AAA Incidence (%)
0.048 0.019
2/11 5/8 1/10
J
Maximal Diameter (mm)
0.036
0.042
K
Elastin Degradation Grade
0.013 0.007
L
non-Dissection
Dissection
Dissection rate (%)
0.046 0.06
1/11 4/8 1/10
M
Relative Apoc3 expression
ns ns
N
Mouse APOC3 (ug/ml)
ns ns
O
Relative hAPOC3 expression
<0.0001
ns
P
Human APOC3 (ug/ml)
P<0.0001
ns
Q
Body weight (g)
ns
Before
After
R
SBP (mmHg)
<0.0001
ns
ns

Figure 7

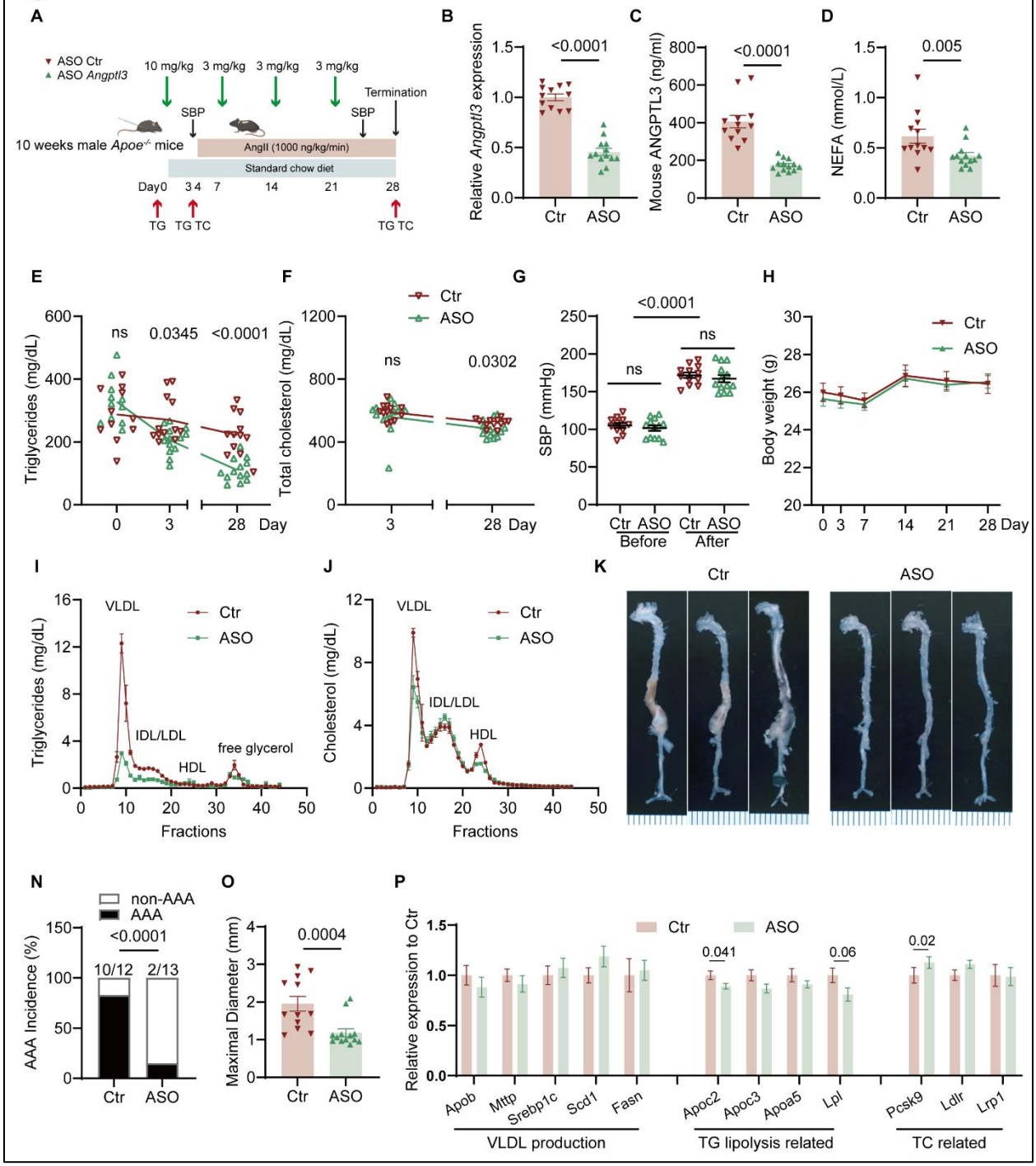
A
ASO Ctr
ASO Angptl3
10 mg/kg
3 mg/kg
3 mg/kg
3 mg/kg
Termination
SBP
SBP
10 weeks male Apoe-/- mice
AngII (1000 ng/kg/min)
Standard chow diet
Day0 3 4 7 14 21 28
TG TG TC
TG TC
B
Relative Angptl3 expression
<0.0001
Ctr ASO
C
Mouse ANGPTL3 (ng/ml)
<0.0001
Ctr ASO
D
NEFA (mmol/L)
0.005
Ctr ASO
E
Triglycerides (mg/dL)
ns 0.0345 <0.0001
0 3 28 Day
F
Total cholesterol (mg/dL)
Ctr
ASO
ns 0.0302
3 28 Day
G
SBP (mmHg)
<0.0001
ns
ns
Ctr ASO Ctr ASO
Before After
H
Body weight (g)
Ctr
ASO
0 3 7 14 21 28 Day
I
Triglycerides (mg/dL)
VLDL
Ctr
ASO
IDL/LDL
HDL
free glycerol
Fractions
J
Cholesterol (mg/dL)
VLDL
Ctr
ASO
IDL/LDL
HDL
Fractions
K
Ctr
ASO
N
non-AAA
AAA
AAA Incidence (%)
<0.0001
10/12 2/13
Ctr ASO
O
Maximal Diameter (mm)
0.0004
Ctr ASO
P
Relative expression to Ctr
Ctr
ASO
0.041
0.06
0.02
Apob Mttp Srebp1c Scd1 Fasn
Apoc2 Apoc3 Apoa5 Lpl
Pcsk9 Ldlr Lrp1
VLDL production
TG lipolysis related
TC related